NATIONAL ADVISORY COMMITTEE FOR AERONAUTICS

TECHNICAL NOTE

No. 1591

AERODYNAMIC CHARACTERISTICS OF A NUMBER OF MODIFIED NACA FOUR-DIGIT-SERIES AIRFOIL SECTIONS

By Laurence K. Loftin, Jr., and Kenneth S. Cohen

Langley Memorial Aeronautical Laboratory
Langley Field, Va.

Washington
June 1948

NATIONAL ADVISORY COMMITTEE FOR AERONAUTICS

TECHNICAL NOTE NO. 1591

AERODYNAMIC CHARACTERISTICS OF A NUMBER OF MODIFIED NACA FOUR-DIGIT-SERIES AIRFOIL SECTIONS

By Laurence K. Loftin, Jr., and Kenneth S. Cohen

SUMMARY

Theoretical pressure distributions have been calculated and the experimental aerodynamic characteristics determined at low speeds for a selected group of the NACA four-digit-series airfoil sections which had previously been modified for high-speed applications. The experimental investigation which was made in the Langley two-dimensional low-turbulence pressure tunnel consisted of measurements of the lift, drag, and pitching-moment characteristics of each of the plain airfoils at Reynolds numbers of 3.0×10^6, 6.0×10^6, and 9.0×10^6. In addition, the effectiveness of flaps when applied to these airfoils and the effect upon the aerodynamic characteristics of standard leading-edge roughness were determined at a Reynolds number of 6.0×10^6. Also tested were three conventional NACA four-digit-series airfoil sections which had not previously been investigated in the Langley two-dimensional low-turbulence pressure tunnel.

The results of the experimental investigation indicated that the maximum lift characteristics of the modified NACA four-digit-series sections having normal-size leading-edge radii and a maximum thickness of 12 percent chord located at 40 percent chord very closely approximated those of smooth NACA 64-series low-drag sections of corresponding thickness and camber. When the leading-edge radius was reduced to one-quarter normal size, the maximum lift coefficients of the 10-percent-thick airfoils with maximum thickness located at 40 and 50 percent chord were about 35 percent lower than those of NACA 64-series sections of corresponding thickness and camber. For airfoils equipped with 20-percent-chord split flaps deflected 60°, the maximum lift of the airfoils with one-quarter normal-size leading-edge radii more nearly approached that of NACA 64-series airfoils. Roughness had no appreciable effect upon the maximum lift of these airfoils. The minimum drag coefficients of the airfoils with maximum thickness at 40 percent chord and normal-size leading-edge radii were higher than those of the corresponding NACA 64-series sections. Reducing the leading-edge radius to one-quarter normal size and moving the position of maximum thickness to 40 and 50 percent chord caused the minimum drag coefficients to be reduced to values about the same as those of corresponding NACA 64- and 66-series sections, respectively. Increases in the trailing-edge angle resulting

from rearward movement of the position of maximum thickness caused sharp decreases in the lift-curve slope and pronounced forward movement of the aerodynamic center.

INTRODUCTION

The increasing demand for high speeds in modern airplanes has focused much attention upon airfoil sections capable of operation at high Mach numbers without suffering the adverse effects of compressibility. One of the first systematic series of airfoil sections developed with a view toward high-speed application consisted of modified NACA four-digit-series sections. Descriptions and high Mach number data obtained in the NACA 11-inch high-speed tunnel were presented in 1934 (reference 1) for these airfoil sections. Since the issuance of reference 1, the modified NACA four-digit-series sections have been employed rather extensively in Europe, particularly in Germany, and have recently received favorable consideration in this country.

Low-speed aerodynamic data obtained in the NACA Variable-Density Wind Tunnel are available for several of the modified NACA four-digit-series airfoil sections (reference 2). The range of airfoil types covered by these data, however, is very limited. In view of the meager amount of data available for the modified NACA four-digit-series sections and because of the recent interest shown in them, an investigation of the low-speed aerodynamic characteristics of a selected group was undertaken in the Langley two-dimensional low-turbulence pressure tunnel. The airfoils chosen for test were those which appeared from theoretical pressure-distribution calculations to offer the best possibilities for high-speed applications. The results of the experimental investigation, together with the theoretical pressure-distribution data for a number of the modified NACA four-digit-series sections, are presented in this paper.

The aerodynamic characteristics of five of the modified sections are presented; three of these are symmetrical and two are cambered with the NACA mean line $a = 0.8$ (modified). (See reference 3.) Also presented are characteristics of three conventional NACA four-digit-series sections, data for which are not included in the systematic results of reference 4 for this series.

COEFFICIENTS AND SYMBOLS

c_d section drag coefficient

$c_{d_{min}}$ minimum section drag coefficient

c_l	section lift coefficient
$c_{l_{max}}$	maximum section lift coefficient
c_{l_i}	design section lift coefficient
$c_{m_{a.c.}}$	section pitching-moment coefficient about aerodynamic center
$c_{m_{c/4}}$	section pitching-moment coefficient about quarter-chord point
α_o	section angle of attack
α_i	section angle of attack corresponding to design lift coefficient
$dc_l/d\alpha$	section lift-curve slope
V	free-stream velocity
v	local velocity
Δv	increment of local velocity
Δv_a	increment of local velocity corresponding to additional type of load distribution
P_R	resultant pressure coefficient; difference between local upper-surface and lower-surface pressure coefficients
R	Reynolds number
R_δ	boundary-layer Reynolds number based on boundary-layer thickness and local velocity outside the boundary layer
c	airfoil chord length
x	distance along chord from leading edge
y	distance perpendicular to chord
y_c	mean-line ordinate
a	mean-line designation, fraction of chord from leading edge over which design load is uniform

DESCRIPTION AND THEORETICAL CHARACTERISTICS OF AIRFOILS

Basic thickness forms.- The modifications to the NACA four-digit-series basic thickness forms, completely described in reference 1, can perhaps be best described here by an explanation of the digits appearing in a typical airfoil designation. Consider, for example, the NACA 0012-64 airfoil section. The first four digits have the usual meaning attached to the numbers appearing in the designation of a conventional NACA four-digit-series airfoil section, in this case a 12-percent-thick symmetrical section. The two numbers following the dash describe the modifications.

The first number following the dash is an index to the size of the leading-edge radius. Leading-edge radii of three sizes, represented by the numbers 3, 6, and 9, were investigated in reference 1. The number 6 which appears in the illustrative example indicates the normal-size leading-edge radius employed with conventional four-digit-series sections; the number 3 represents a one-quarter normal-size leading-edge radius; and the number 9 indicates a leading-edge radius of three times normal size. The second number following the dash indicates the position of maximum thickness in tenths of the chord. Airfoils, which were derived in reference 1, have the position of maximum thickness located at 40, 50, and 60 percent chord.

In order to provide some basis upon which to choose the airfoils to be tested, theoretical pressure distributions were calculated by the methods of reference 5 for a group of modified NACA four-digit-series basic thickness forms. The results of these calculations are presented in figures 1 to 8 for the following airfoil sections:

	NACA 0010-64	NACA 0012-64
	NACA 0010-65	
	NACA 0010-66	
NACA 0008-34	NACA 0010-34	NACA 0012-34
	NACA 0010-35	

In addition to pressure distributions at zero lift, these data include incremental velocity ratios from which the pressure distribution at any lift coefficient may be calculated. The method of making this calculation is described in reference 4.

From the data of figures 1 to 8, the effect upon the pressure distribution of variations in the position of maximum thickness and size of the leading-edge radius are clearly evident. A decrease in both the peak negative pressure coefficient and in the variations of pressure over the forward part of the airfoil is effected by maintaining a normal-size leading-edge radius and moving the position of maximum thickness from 30 (original position) to 40 percent chord (fig. 2).

Further rearward movement of the position of maximum thickness, however, appears to cause a second peak in the pressure distribution near the trailing edge (figs. 3 and 4) followed by a rather sharp, undesirable pressure recovery. With one-quarter normal-size leading-edge radius, the magnitude of the peak negative pressure coefficient is not changed much but its position is moved to the rear. The change in position of minimum pressure is particularly marked when the position of maximum thickness is moved from 40 percent to 50 percent of the chord (figs. 5 and 6). This movement of the position of maximum thickness decreases the peak negative pressure coefficient slightly but results in an undesirably large pressure recovery near the trailing edge. On the basis of these theoretical data and from a consideration of the probable low-speed characteristics, the NACA 0010-34, 0010-35, and 0012-64 basic thickness forms were chosen for tests. The NACA 0010-34 and 0012-64 were also tested in combination with a cambered mean line.

Mean line.- In the present investigation, the modified NACA four-digit-series basic thickness forms which were cambered employed the NACA $a = 0.8$ (modified) mean line (reference 3). This mean line is designed to have a uniform load distribution from the leading edge to the 80-percent-chord station and designed to be geometrically straight from about 85 percent chord to the trailing edge. The NACA $a = 0.8$ (modified) mean line was used because the peak induced velocities added by this mean line to the velocities over the basic thickness form are less than those associated with the older mean lines, such as the NACA 230 and 24 mean line; and the curvature of the airfoil surfaces near the trailing edge which results from the use of an NACA $a = 1.0$ mean line is eliminated.

Ordinates and load-distribution data corresponding to a design lift coefficient of 1.0 are presented in figure 9 for the NACA $a = 0.8$ (modified) mean line. If the ordinates and load are desired for a design lift coefficient other than 1.0, they may be obtained easily by linearly scaling the values presented. The method for combining the pressure-distribution data for the basic thickness forms and mean line to give the pressure distribution about a cambered airfoil at any lift coefficient is given in reference 4.

Designation of cambered airfoil sections.- The method of designating modified NACA four-digit-series airfoil sections which employ the NACA $a = 0.8$ (modified) mean line is illustrated by the following example:

NACA 0012-64, $a = 0.8$ (modified), $c_{l_i} = 0.2$

This system of numbers designates an NACA 0012-64 basic thickness form laid off on an NACA $a = 0.8$ (modified) mean line cambered for a design lift coefficient of 0.2.

Conventional NACA four-digit-series airfoil sections.- Complete descriptions of the basic thickness forms and mean lines of the conventional NACA four-digit-series airfoil sections of which three were tested in the present investigation may be found in references 4 and 6.

APPARATUS AND TESTS

Wind tunnel.- The experimental investigation was made in the Langley two-dimensional low-turbulence pressure tunnel. The test section of this tunnel measures 3 feet by 7.5 feet with the models, when mounted, completely spanning the 3-foot dimension and with the juncture between the model and tunnel walls sealed to prevent air leakage. Lift measurements were made by taking the difference between the pressure reaction upon the floor and ceiling of the tunnel, drag measurements were made by the wake-survey method, and pitching moments were determined with a torque balance. A more complete description of the tunnel and the methods of obtaining and reducing the data are contained in reference 7.

Models.- The eight airfoil sections for which the experimental aerodynamic characteristics were obtained are:

NACA 0010-35
NACA 0010-34, a = 0.8 (modified), $c_{l_i} = 0.2$

NACA 0012
NACA 0012-64, a = 0.8 (modified), $c_{l_i} = 0.2$

NACA 2408
NACA 2410

The models representing the airfoil sections were of 24-inch chord and, with the exception of the 8-percent-thick section which was machined from steel, were constructed of laminated mahogany. The models were sprayed with lacquer and then sanded with No. 400 carborundum paper until aerodynamically smooth surfaces were obtained. The ordinates of the models tested are presented in table I.

Tests.- The tests of each smooth airfoil section consisted of measurements of the lift, drag, and quarter-chord pitching moment at Reynolds numbers of 3.0×10^6, 6.0×10^6, and 9.0×10^6. In addition, the lift and drag characteristics of each section were determined at a Reynolds number of 6.0×10^6 with standard roughness applied to the leading edge of the model. The standard roughness employed on these

24-inch-chord models consisted of 0.011-inch-diameter carborundum grains spread over a surface length of 8 percent of the chord back from the leading edge on the upper and lower surfaces. The grains were thinly spread to cover from 5 to 10 percent of this area. In an effort to gain some idea of the effectiveness of flaps when applied to these airfoils, each airfoil was fitted with a 0.20c simulated split flap deflected 60°. Lift measurements were made at a Reynolds number of 6.0×10^6 with the split flap, with the airfoil leading edge both smooth and rough.

RESULTS

The results obtained from tests of the eight airfoil sections are presented (figs. 10 to 17) as plots of standard aerodynamic coefficients representing the lift, drag, and quarter-chord pitching-moment characteristics of the airfoil sections. The position of the aerodynamic center, as determined from the experimental results, and the variation of the pitching-moment coefficient about this point are also included. The influence of the tunnel boundaries has been removed from all the aerodynamic data by means of the following equations (developed in reference 7):

$$c_d = 0.990\ c_d'$$

$$c_l = 0.973\ c_l'$$

$$c_{m_{c/4}} = 0.951\ c_{m_{c/4}}'$$

$$\alpha_o = 1.015\ \alpha_o'$$

where the primed quantities represent the measured coefficients.

DISCUSSION

The discussion is primarily concerned with an analysis of the effects, as shown by tests of the five modified NACA four-digit-series airfoil sections, of variations in the leading-edge radius and position of maximum thickness upon the aerodynamic characteristics. In this analysis, frequent use is made of cross plots (figs. 18 to 21) showing the characteristics of the modified sections as compared with those of the conventional NACA four-digit-series sections and NACA 6-series low-drag sections. The comparative results for the NACA 6-series and four-digit-series sections are shown in the form of curves representing faired data taken from reference 4, whereas the results of the present

investigation appear in the cross plots as experimental points. Little mention is made of the results obtained for the three conventional NACA four-digit-series sections tested inasmuch as they follow closely the trends indicated in reference 4 for this series of airfoil sections.

Drag

Minimum drag.- The previously mentioned influence upon the pressure gradients over the forward part of the airfoil of a reduction in size of the leading-edge radius and a rearward movement of the position of maximum thickness has, as might be expected, a favorable effect upon the value of the minimum drag coefficient. An indication of the magnitude of this effect may be gained from figure 18, which shows the minimum section drag coefficient corresponding to a Reynolds number of 6.0×10^6 as a function of airfoil thickness ratio for the five modified NACA four-digit series airfoils, for the conventional NACA four-digit series, and for the NACA 64- and 66-series low-drag airfoils.

In the smooth condition, the minimum drag of the 10-percent-thick airfoils having leading-edge radii of one-quarter normal size and maximum thickness at 40 and 50 percent chord was of the same order, respectively, as that obtained for NACA 64- and 66-series low-drag airfoils of comparable thickness. This similarity in drag indicates the existence of considerable laminar flow over the airfoil surfaces. The small, though rather extensive, positive pressure gradient, which occurs over the surfaces of the 12-percent-thick airfoils having leading-edge radii of normal size and maximum thickness at 40 percent chord, gives rise to a minimum drag coefficient which lies between those of the NACA 64-series low-drag section and NACA four-digit-series section of comparable thickness. The addition of the NACA $a = 0.8$ (modified) mean line to the NACA 0010-34 and 0012-64 basic thickness forms does not appreciably affect the value of the minimum drag coefficient. The faired data of reference 4, which are presented in figure 18, indicate that airfoil thickness form and mean line have little effect upon the value of the minimum drag coefficient when the airfoil leading edges are in the rough condition; and the results of the present investigation (fig. 18) follow the same trend.

The airfoil basic thickness distribution appears to have a marked effect upon the manner in which the minimum drag coefficient varies with Reynolds number (figs. 10 to 14). The controlling action of the airfoil pressure distribution upon the extent to which the opposite effects of a thinning boundary layer and a forward movement of the point of transition balance each other as the Reynolds number is increased suggests itself as a possible explanation. Some insight into the mechanism by which the airfoil pressure distribution influences the movement of the transition point with Reynolds number may be gained from the theoretical work of Schlichting and Ulrich (reference 8).

The results of this work show the existence of a critical boundary-layer Reynolds number $R_{\delta_{crit}}$ above which the laminar boundary layer is no longer stable and may become turbulent. Furthermore, the value of the critical boundary-layer Reynolds number is shown to decrease rapidly and the laminar boundary layer to become increasingly unstable as the pressure gradient along the surface becomes positive. In the presence of an unfavorable pressure gradient, the transition point is, therefore, most likely to move rapidly forward once the critical boundary-layer Reynolds number has been reached.

In consideration of the ideas of Schlicting and Ulrich in relation to the increase of minimum drag with Reynolds number shown by the NACA 0012-64 section (fig. 13), the unfavorable pressure gradient over this airfoil (fig. 8) would seem to be responsible for a rapid forward movement of transition which overbalances the normal thinning of the boundary layer and consequent reduction in drag that usually accompany an increase in Reynolds number. On the other hand, the NACA 0010-34 (fig. 10) and NACA 0010-35 (fig. 12) airfoils which possess more favorable pressure gradients have a negligible scale effect between Reynolds numbers of 3.0×10^6 and 9.0×10^6. This fact indicates that the opposite effects of a thinning boundary layer and a forward movement of transition nearly counterbalance each other. The uniformly favorable influence upon the minimum drag of NACA 6-series sections of increasing the Reynolds number from 3.0×10^6 to 9.0×10^6 indicates that $R_{\delta_{crit}}$ of these airfoil sections, which have marked negative pressure gradients, is sufficiently high so that no appreciable forward movement of transition occurs between these Reynolds numbers; and, thus, the favorable effect of a thinning boundary layer predominates.

Low-drag range.- The range of lift coefficients over which low drag is obtained and the manner in which this range varies with Reynolds number are about the same for the NACA 0010-34 and 0010-35 airfoil sections (figs. 10 and 12) as for the NACA 6-series sections of comparable thickness (reference 4). The low-drag range for the NACA 0012-64 section (fig. 13), however, is quite small at a Reynolds number of 3.0×10^6 and is practically nonexistent at a Reynolds number of 9.0×10^6. The more positive pressure gradients on the NACA 0012-64 section are probably responsible for the behavior of the low-drag range on this airfoil section.

The relationship between the drag and lift outside the low-drag range of lift coefficients is about the same for the NACA 0010-34 and NACA 0012-64 airfoils, both cambered and uncambered, as for the NACA 64-series low-drag sections of comparable thickness; a somewhat less marked correspondence exists between the drag characteristics of the NACA 0010-35 section and a comparable NACA 66-series low-drag section. These comparisons are valid for the airfoils in both the smooth and rough conditions.

Lift

Lift-curve slope.- Rearward movement of the position of maximum thickness of the NACA four-digit-series sections is accompanied by an increase in trailing-edge angle. In accordance with previous experimental work (references 9 and 10), the lift-curve slope decreases with increasing trailing-edge angle. The results of the present investigation (fig. 19) for the 10-percent-thick and 12-percent-thick sections having maximum thickness at various positions indicate the same trend, with the greatest decrease in the lift-curve slope being about 16 percent.

From theoretical considerations, the lift-curve slope should increase with increasing airfoil thickness ratio; and the comparative data from reference 4 (fig. 19) for NACA 64-series low-drag sections, which have very small trailing-edge angles, indicate that such is the case. If, however, the trailing-edge angle is large and increases rapidly with increasing airfoil thickness ratio, the theoretical increase in lift-curve slope with thickness will be overbalanced by the opposite effect of increasing trailing-edge angle. The NACA four-digit series sections, data for which are presented in figure 19, have this characteristic. Since, with increasing thickness, the trailing-edge angles of the modified NACA four-digit-series sections become progressively larger than those of the conventional NACA four-digit-series sections, a more rapid decrease in lift-curve slope with increasing thickness would be expected for these modified airfoils. The amount of data available for the modified NACA four-digit-series sections does not appear to be sufficient, however, to define adequately this trend or to permit any definite statements as to the relative effects of roughness on the lift-curve slopes of the modified and conventional NACA four-digit-series sections.

Angle of zero lift.- There appears to be no appreciable difference in the section angles of zero lift of the NACA 0010-34 and NACA 0012-64 airfoil sections cambered with the NACA $a = 0.8$ (modified) mean line (figs. 11 and 14). The values are slightly more negative than those predicted from the theoretical mean-line data presented in figure 9 but agree quite well with the experimental values obtained for cambered NACA 6A-series airfoil sections employing the NACA $a = 0.8$ (modified) mean line (reference 3).

Maximum lift.- Some idea of the effect upon the maximum lift coefficient of variations of the position of maximum thickness and leading-edge radius may be gained from figure 20. This figure shows the maximum section lift coefficients ($R = 6.0 \times 10^6$) for the modified NACA four-digit-series airfoils as a function of airfoil thickness ratio, with comparative data from reference 4 for NACA 64-series low-drag airfoils. As might be expected from previous investigations, the lowest maximum lift coefficients were obtained for the airfoils having one-quarter normal-size leading-edge radii. The maximum lift coefficients of the two symmetrical sections (NACA 0010-34 and 0010-35) are about the same and do not appear to vary as the leading-edge condition is changed

from smooth to rough. These results show that if the leading edge is sufficiently sharp, the usual important influence of surface condition is negligible. The extremely low value of the maximum lift obtained under these conditions is shown by comparison with results for the NACA 64-010 section. The maximum lift coefficients of the two modified NACA four-digit-series sections are about 35 percent lower than that of the NACA 64-010 section in the smooth condition and about 15 percent lower when the leading edges of the airfoils are rough. The increment in maximum lift caused by cambering the NACA 0010-34 section is about the same as that observed for the addition of approximately the same amount of camber to the NACA 64-010 section. Even with camber, the maximum lift of the NACA 0010-34 section is about 23 percent lower than that of the NACA 64-010 section; but with rough leading edge, the NACA 64-010 section has a maximum lift coefficient which is about the same as that of the cambered NACA 0010-34 section.

The maximum lift of the three airfoils having one-quarter normal-size leading-edge radii with smooth leading edges and equipped with 0.20c split flaps deflected 60°, more nearly approaches that of NACA 64-series low-drag sections of corresponding thickness and camber. The decrement in maximum lift coefficient caused by leading-edge roughness is, however, so small for these three sections that in the rough condition the maximum lift of the three modified NACA four-digit-series sections is as good as or better than that of corresponding NACA 64-series airfoils.

Moving the position of maximum thickness from 30 percent to 40 percent chord while maintaining a normal-size leading-edge radius reduces the maximum lift coefficient of the plain airfoil about 15 percent, as shown by the comparative data for the NACA 0012 and NACA 0012-64 sections. Clearly illustrated here is the important point that a reduction in thickness of the airfoil near the leading edge, such as occurred in this case, has a definitely adverse effect upon the maximum lift coefficient although the leading-edge radius itself may not be decreased. The maximum lift coefficients of the cambered and symmetrical NACA 0012-64 airfoil sections in both the smooth condition and with standard leading-edge roughness are nearly the same as those of the corresponding cambered and symmetrical NACA 64-series low-drag sections (fig. 20).

The value of the maximum lift coefficient presented in figure 20 for the NACA 0012-64 section is about 13 percent lower than that indicated by tests of the same airfoil in the NACA Variable-Density Wind Tunnel (reference 2). The value obtained in the present investigation, however, was very carefully checked and is believed to be correct. The discrepancy between the values obtained in the two tunnels may possibly have been caused by turbulence effects not fully accounted for on this sensitive airfoil by the effective Reynolds number correction applied to the Variable-Density Wind-Tunnel results.

The results presented in figure 20 show that, in the smooth condition at least, the maximum lift coefficients of the cambered and symmetrical NACA 0012-64 airfoil sections, when equipped with 0.20c split flaps deflected 60°, are somewhat higher than those of corresponding NACA 64-series sections. This result may be explained by the fact that the trailing-edge angle of the NACA 0012-64 airfoil is larger than that of the NACA 64-012 airfoil since the experimental results presented in reference 3 indicate a slight improvement in the maximum lift of NACA 6-series sections with split flaps when the trailing-edge cusp is removed. The results for the cambered and symmetrical NACA 0012-64 airfoil with rough leading edges do not form a consistent comparison with results for the NACA 64-series sections. In neither case, however, is the modified NACA four-digit-series section worse than the corresponding NACA 64-series airfoil.

Between Reynolds numbers of 3.0×10^6 and 9.0×10^6, none of the modified NACA four-digit-series sections show any appreciable scale effect on maximum lift.

Pitching Moment

Quarter-chord point.- The two airfoils cambered with the NACA $a = 0.8$ (modified) mean line have quarter-chord pitching moments (figs. 11 and 14) which agree closely with those predicted from the theoretical pitching-moment data (fig. 9).

Aerodynamic center.- The chordwise position of the aerodynamic center for the modified NACA four-digit-series sections is shown in figure 21 as a function of airfoil thickness ratio, together with similar data taken from reference 4 for the conventional NACA four-digit-series sections and the NACA 64-series low-drag sections. The forward movement of the aerodynamic center which is seen to accompany rearward movement of the position of maximum thickness on the modified NACA four-digit-series sections is in agreement with the trends of reference 11 which show that such a forward movement follows an increase in trailing-edge angle. Theoretical considerations indicate a rearward movement of the aerodynamic center with increasing airfoil thickness ratio, and the data for NACA 64-series sections follow this trend; but the effect of increasing trailing-edge angle predominates in the case of the conventional NACA four-digit-series sections as evidenced by the forward movement of the aerodynamic center. (See fig. 20.) Since the trailing-edge angles of the modified NACA four-digit-series sections become progressively larger with increasing airfoil thickness than those of the conventional NACA four-digit-series sections, a more pronounced forward movement of the aerodynamic center with increasing thickness would be expected for these airfoil sections; and the comparative results for the NACA 0012-64 and 0010-34 sections seem to show this trend.

CONCLUSIONS

Based upon a two-dimensional investigation of the aerodynamic characteristics of five modified NACA four-digit-series airfoil sections at Reynolds numbers from 3.0×10^6 to 9.0×10^6, the following conclusions may be drawn:

1. The maximum lift characteristics of the airfoil sections having normal-size leading-edge radii and a maximum thickness of 12 percent chord located at 40 percent chord very closely approximated those of NACA 64-series low-drag sections of corresponding thickness and camber.

2. The maximum lift coefficients of the 10-percent-thick airfoils with one-quarter normal-size leading-edge radii and maximum thickness located at 40 and 50 percent chord were about 35 percent lower than those of smooth NACA 64-series sections of corresponding thickness and camber. For airfoils equipped with 20-percent-chord split flaps deflected 60°, the maximum lift of the airfoils with one-quarter normal-size leading-edge radii more nearly approached that of NACA 64-series airfoils. Roughness had no appreciable effect upon the maximum lift of these airfoils.

3. The minimum drag coefficients of the airfoils with maximum thickness at 40 percent chord and normal-size leading-edge radii were higher than those of the corresponding NACA 64-series sections. Reducing the leading-edge radius to one-quarter normal size and moving the position of maximum thickness to 40 and 50 percent chord caused the minimum drag coefficients to be reduced to values about the same as those for corresponding NACA 64- and 66-series sections, respectively.

4. Increases in the trailing-edge angle resulting from rearward movement of the position of maximum thickness caused sharp decreases in the lift-curve slope and pronounced forward movements of the aerodynamic center.

Langley Memorial Aeronautical Laboratory
National Advisory Committee for Aeronautics
Langley Field, Va., October 1, 1947

REFERENCES

1. Stack, John, and von Doenhoff, Albert E.: Tests of 16 Related Airfoils at High Speeds. NACA Rep. No. 492, 1934.

2. Jacobs, Eastman N., Pinkerton, Robert M., and Greenberg, Harry: Tests of Related Forward-Camber Airfoils in the Variable-Density Wind Tunnel. NACA Rep. No. 610, 1937.

3. Loftin, Laurence K., Jr.: Theoretical and Experimental Data for a Number of NACA 6A-Series Airfoil Sections. NACA TN No. 1368, 1947.

4. Abbott, Ira H., von Doenhoff, Albert E., and Stivers, Louis S., Jr.: Summary of Airfoil Data. NACA ACR No. L5C05, 1945.

5. Theodorsen, Theodore: Theory of Wing Sections of Arbitrary Shape. NACA Rep. No. 411, 1931.

6. Jacobs, Eastman N., Ward, Kenneth E., and Pinkerton, Robert M.: The Characteristics of 78 Related Airfoil Sections from Tests in the Variable-Density Wind Tunnel. NACA Rep. No. 460, 1933.

7. von Doenhoff, Albert E., and Abbott, Frank T., Jr.: The Langley Two-Dimensional Low-Turbulence Pressure Tunnel. NACA TN No. 1283, 1947.

8. Schlichting, H., and Ulrich, A.: Zur Berechnung des Umschlages laminar turbulent. Jahrb. 1942 der deutschen Luftfahrtforschung, R. Oldenbourg (Munich), pp. I 8 – I 35.

9. Purser, Paul E., and McKee, John W.: Wind-Tunnel Investigation of a Plain Aileron with Thickened and Beveled Trailing Edges on a Tapered Low-Drag Wing. NACA ACR, Jan. 1943.

10. Jones, Robert T., and Ames, Milton B., Jr.: Wind-Tunnel Investigation of Control-Surface Characteristics. V – The Use of a Beveled Trailing Edge to Reduce the Hinge Moment of a Control Surface. NACA ARR, March 1942.

11. Purser, Paul E., and Johnson, Harold S.: Effects of Trailing-Edge Modifications on Pitching-Moment Characteristics of Airfoils. NACA CB No. L4130, 1944.

TABLE I

ORDINATES OF NACA AIRFOIL SECTIONS TESTED

NACA 0010-34

[Stations and ordinates given in percent of airfoil chord]

Upper Surface		Lower Surface	
Station	Ordinate	Station	Ordinate
0	0	0	0
.75	.714	.75	-.714
1.25	.944	1.25	-.944
2.5	1.400	2.5	-1.400
5.0	2.078	5.0	-2.078
7.5	2.611	7.5	-2.611
10	3.044	10	-3.044
15	3.744	15	-3.744
20	4.244	20	-4.244
30	4.833	30	-4.833
40	5.000	40	-5.000
50	4.856	50	-4.856
60	4.433	60	-4.433
70	3.733	70	-3.733
80	2.767	80	-2.767
90	1.556	90	-1.556
95	.856	95	-.856
100	.100	100	-.100

L.E. radius: 0.272

NACA 0010-34
a = 0.8 (modified), $c_{l_i} = 0.2$

[Stations and ordinates given in percent of airfoil chord]

Upper Surface		Lower Surface	
Station	Ordinate	Station	Ordinate
0	0	0	0
.687	.790	.813	-.632
1.176	1.062	1.324	-.820
2.407	1.608	2.593	-1.186
4.887	2.436	5.113	-1.714
7.378	3.094	7.622	-2.122
9.875	3.637	10.125	-2.445
14.876	4.523	15.124	-2.961
19.886	5.172	20.114	-3.312
29.917	5.980	30.083	-3.684
39.955	6.279	40.045	-3.721
49.994	6.186	50.006	-3.526
60.031	5.735	59.969	-3.131
70.064	4.915	69.936	-2.549
80.100	3.700	79.900	-1.830
90.076	2.044	89.924	-1.064
95.042	1.100	94.958	-.610
100.000	.100	100.000	-.100

L.E. radius: 0.272
Slope of radius through L.E.: 0.095

NACA 0012-64

[Stations and ordinates given in percent of airfoil chord]

Upper Surface		Lower Surface	
Station	Ordinate	Station	Ordinate
0	0	0	0
1.25	1.813	1.25	-1.813
2.5	2.453	2.5	-2.453
5.0	3.267	5.0	-3.267
7.5	3.813	7.5	-3.813
10	4.240	10	-4.240
15	4.867	15	-4.867
20	5.293	20	-5.293
30	5.827	30	-5.827
40	6.000	40	-6.000
50	5.827	50	-5.827
60	5.320	60	-5.320
70	4.480	70	-4.480
80	3.320	80	-3.320
90	1.867	90	-1.867
95	1.027	95	-1.027
100	.120	100	-.120

L.E. radius: 1.582

NACA 0012-64
a = 0.8 (modified), $c_{l_i} = 0.2$

[Stations and ordinates given in percent of airfoil chord]

Upper Surface		Lower Surface	
Station	Ordinate	Station	Ordinate
0	0	0	0
1.107	1.928	1.393	-1.686
2.336	2.659	2.664	-2.237
4.823	3.623	5.177	-2.901
7.322	4.295	7.678	-3.323
9.825	4.832	10.175	-3.640
14.839	5.645	15.161	-4.083
19.858	6.221	20.142	-4.361
29.900	6.974	30.100	-4.678
39.946	7.279	40.054	-4.721
49.993	7.157	50.007	-4.497
60.038	6.622	59.962	-4.018
70.077	5.662	69.923	-3.296
80.120	4.253	79.880	-2.383
90.091	2.355	89.909	-1.375
95.050	1.271	94.950	-.781
100.000	.120	100.000	-.120

L.E. radius: 1.582
Slope of radius through L.E.: 0.095

TABLE I - Concluded

ORDINATES OF NACA AIRFOIL SECTIONS TESTED

NACA 0010-35

[Stations and ordinates given in percent of airfoil chord]

Upper Surface		Lower Surface	
Station	Ordinate	Station	Ordinate
0	0	0	0
.75	.674	.75	-.674
1.25	.878	1.25	-.878
2.5	1.267	2.5	-1.267
5.0	1.844	5.0	-1.844
7.5	2.289	7.5	-2.289
10	2.667	10	-2.667
15	3.289	15	-3.289
20	3.789	20	-3.789
30	4.478	30	-4.478
40	4.878	40	-4.878
50	5.000	50	-5.000
60	4.867	60	-4.867
70	4.389	70	-4.389
80	3.500	80	-3.500
90	2.100	90	-2.100
95	1.178	95	-1.178
100	.100	100	-.100
L.E. radius: 0.272			

NACA 0012

[Stations and ordinates given in percent of airfoil chord]

Upper Surface		Lower Surface	
Station	Ordinate	Station	Ordinate
0	0	0	0
1.25	1.894	1.25	-1.894
2.5	2.615	2.5	-2.615
5.0	3.555	5.0	-3.555
7.5	4.200	7.5	-4.200
10	4.683	10	-4.683
15	5.345	15	-5.345
20	5.738	20	-5.738
25	5.941	25	-5.941
30	6.002	30	-6.002
40	5.803	40	-5.803
50	5.294	50	-5.294
60	4.563	60	-4.563
70	3.664	70	-3.664
80	2.623	80	-2.623
90	1.448	90	-1.448
95	.807	95	-.807
100	.126	100	-.126
L.E. radius: 1.58			

NACA 2408

[Stations and ordinates given in percent of airfoil chord]

Upper Surface		Lower Surface	
Station	Ordinate	Station	Ordinate
0	0	0	0
1.128	1.380	1.372	-1.134
2.337	1.977	2.663	-1.493
4.794	2.829	5.206	-1.891
7.273	3.471	7.727	-2.111
9.768	3.987	10.232	-2.237
14.778	4.776	15.222	-2.338
19.809	5.320	20.191	-2.320
24.852	5.677	25.148	-2.239
29.900	5.875	30.100	-2.125
40.000	5.869	40.000	-1.869
50.039	5.473	49.961	-1.585
60.068	4.820	59.932	-1.264
70.081	3.942	69.919	-.942
80.078	2.858	79.922	-.636
90.054	1.575	89.946	-.353
95.033	.855	94.967	-.217
100.000	.084	100.000	-.084
L.E. radius: 0.70 Slope of radius through L.E.: 0.1			

NACA 2410

[Stations and ordinates given in percent of airfoil chord]

Upper Surface		Lower Surface	
Station	Ordinate	Station	Ordinate
0	0	0	0
1.098	1.694	1.402	-1.148
2.297	2.411	2.703	-1.927
4.742	3.420	5.258	-2.482
7.217	4.169	7.783	-2.809
9.710	4.766	10.290	-3.016
14.722	5.665	15.278	-3.227
19.761	6.276	20.239	-3.276
24.814	6.668	25.186	-3.230
29.875	6.875	30.125	-3.125
40.000	6.837	40.000	-2.837
50.049	6.356	49.951	-2.468
60.085	5.580	59.915	-2.024
70.102	4.551	69.898	-1.551
80.097	3.296	79.903	-1.074
90.067	1.816	89.933	-.594
95.041	.990	94.959	-.352
100.000	.105	100.000	-.105
L.E. radius: 1.10 Slope of radius through L.E.: 0.1			

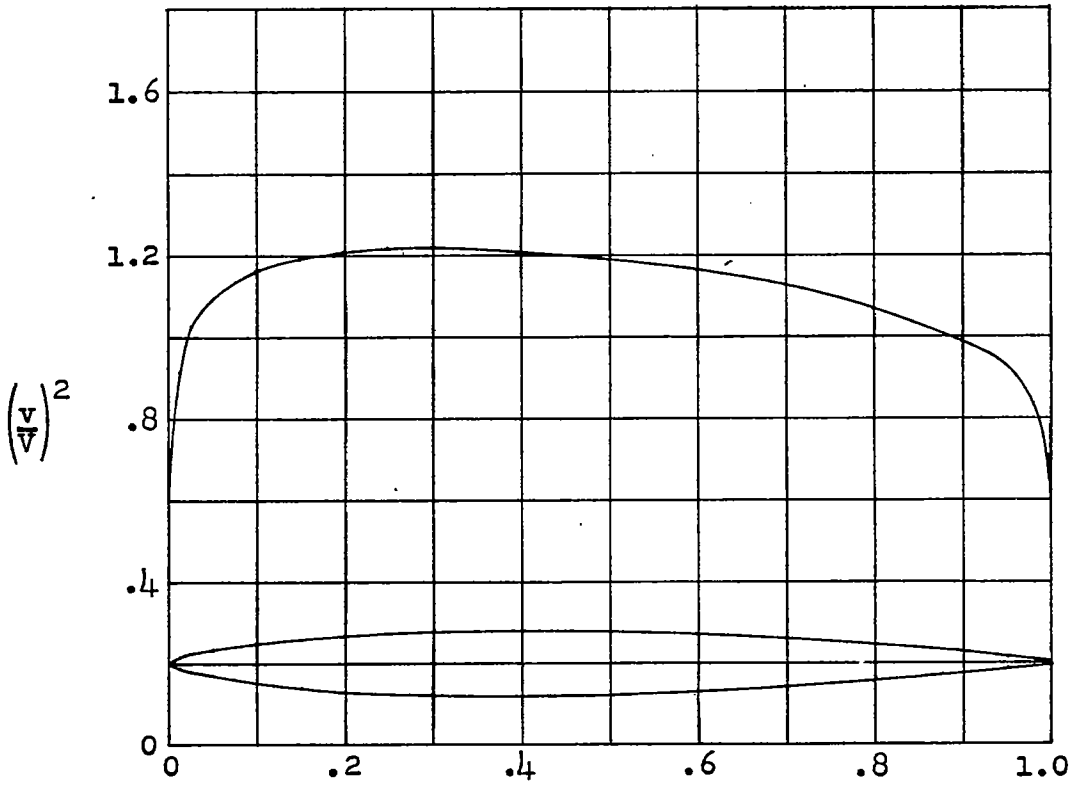

x (percent c)	y (percent c)	$(v/V)^2$	v/V	$\Delta v_a/V$
0	0	0	0	4.839
1.25	.756	.917	.958	1.338
2.5	1.120	1.023	1.011	.966
5.0	1.662	1.092	1.045	.691
7.5	2.089	1.137	1.066	.564
10	2.436	1.162	1.078	.485
15	2.996	1.188	1.090	.387
20	3.396	1.206	1.098	.326
30	3.867	1.217	1.103	.248
40	4.000	1.202	1.096	.197
50	3.884	1.185	1.089	.157
60	3.547	1.163	1.079	.128
70	2.987	1.127	1.062	.100
80	2.213	1.067	1.033	.074
90	1.244	.993	.996	.047
95	.684	.932	.965	.031
100	.080	0	0	0
L.E. radius: 0.174 percent c				

Figure 1.- NACA 0008-34 basic thickness form.

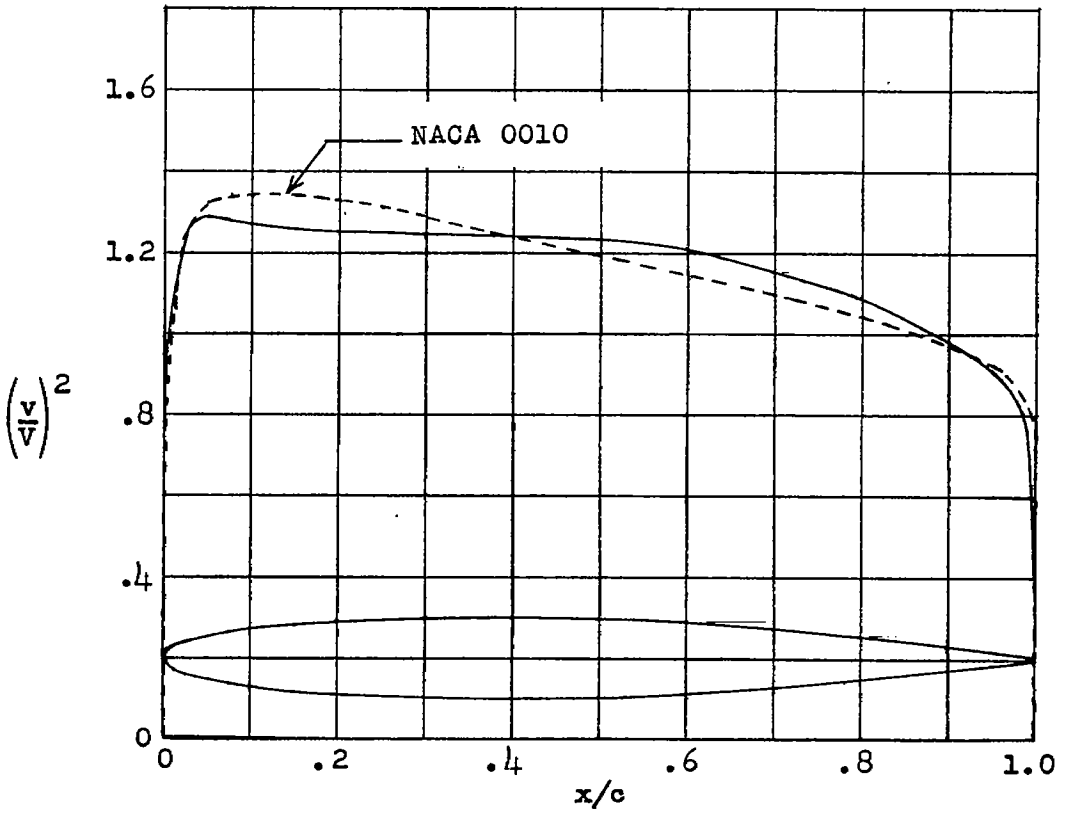

x (percent c)	y (percent c)	$(v/V)^2$	v/V	$\Delta v_a/V$
0	0	0	0	2.324
1.25	1.511	1.108	1.053	1.286
2.5	2.044	1.245	1.116	.966
5.0	2.722	1.286	1.134	.690
7.5	3.178	1.277	1.130	.556
10	3.533	1.269	1.127	.475
15	4.056	1.261	1.123	.377
20	4.411	1.248	1.117	.316
30	4.856	1.244	1.116	.241
40	5.000	1.242	1.115	.193
50	4.856	1.231	1.110	.155
60	4.433	1.211	1.101	.126
70	3.733	1.155	1.074	.098
80	2.767	1.089	1.043	.072
90	1.556	.980	.990	.045
95	.856	.912	.955	.030
100	.100	0	0	0
L.E. radius: 1.10 percent c				

Figure 2.- NACA 0010-64 basic thickness form.

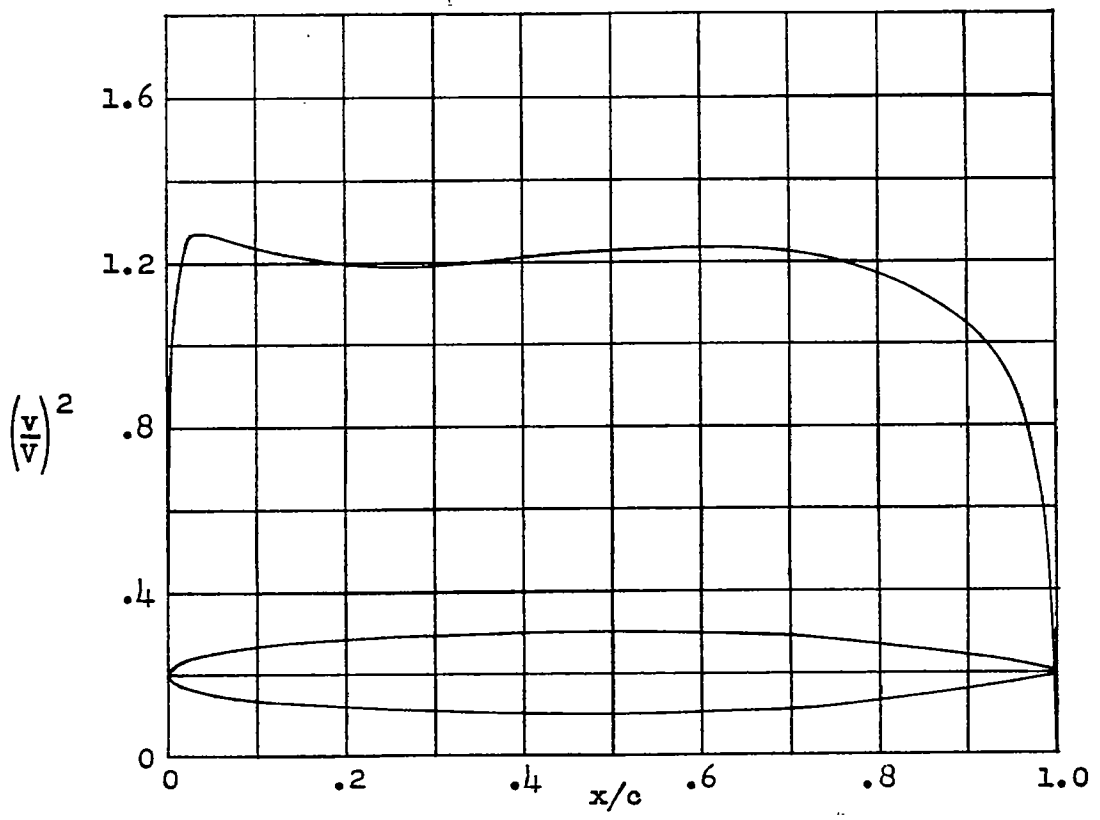

x (percent c)	y (percent c)	$(v/V)^2$	v/V	$\Delta v_a/V$
0	0	0	0	2.584
1.25	1.467	1.140	1.068	1.295
2.5	1.967	1.273	1.128	.970
5.0	2.589	1.271	1.127	.684
7.5	2.989	1.252	1.119	.551
10	3.300	1.236	1.112	.470
15	3.756	1.213	1.101	.372
20	4.089	1.200	1.095	.312
30	4.578	1.196	1.094	.239
40	4.889	1.212	1.101	.193
50	5.000	1.229	1.109	.158
60	4.867	1.234	1.111	.128
70	4.389	1.226	1.107	.103
80	3.500	1.173	1.083	.076
90	2.100	1.049	1.024	.046
95	1.178	.915	.957	.029
100	.100	0	0	0
L.E. radius: 1.10 percent c				

Figure 3.- NACA 0010-65 basic thickness form.

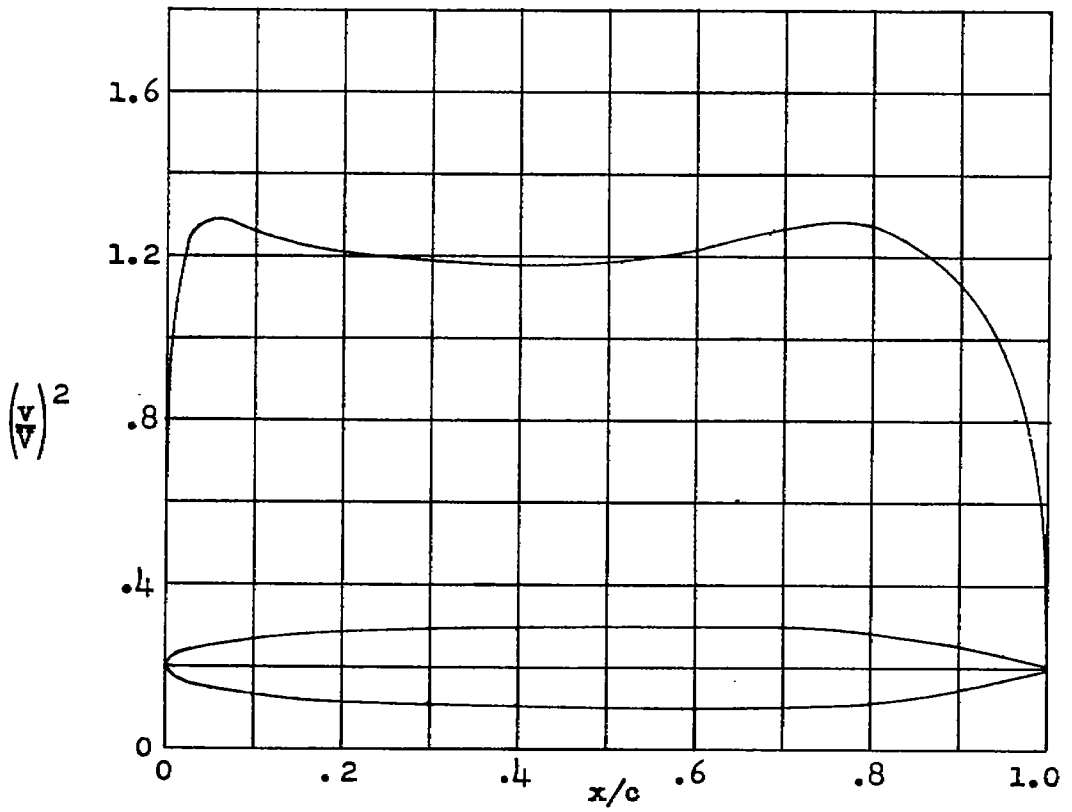

x (percent c)	y (percent c)	$(v/V)^2$	v/V	$\Delta v_a/V$
0	0	0	0	2.434
1.25	1.489	1.130	1.063	1.289
2.5	2.011	1.246	1.116	.959
5.0	2.656	1.286	1.134	.687
7.5	3.089	1.282	1.132	.554
10	3.400	1.258	1.122	.471
15	3.856	1.225	1.107	.372
20	4.178	1.209	1.100	.310
30	4.578	1.189	1.090	.236
40	4.822	1.178	1.085	.190
50	4.956	1.184	1.088	.153
60	5.000	1.214	1.102	.129
70	4.889	1.265	1.125	.104
80	4.300	1.278	1.130	.080
90	2.833	1.135	1.065	.049
95	1.656	.960	.980	.030
100	.100	0	0	0
L.E. radius: 1.10 percent c				

Figure 4.- NACA 0010-66 basic thickness form.

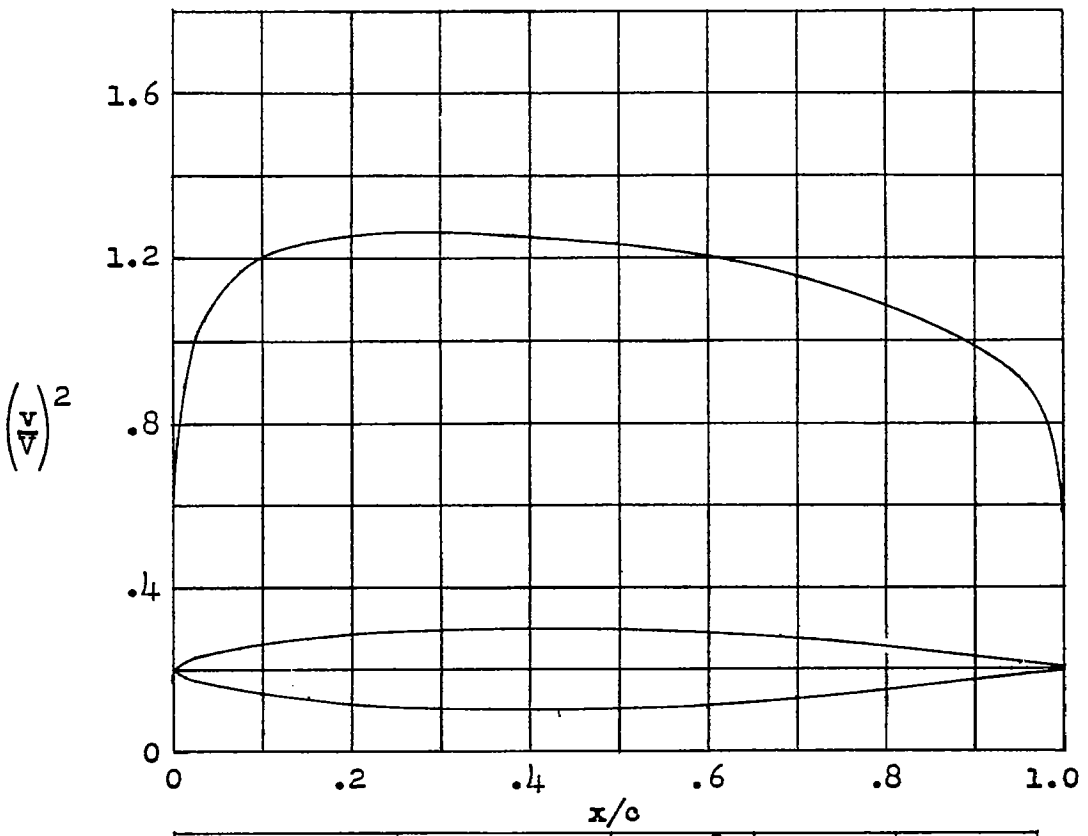

x (percent c)	y (percent c)	$(v/V)^2$	v/V	$\Delta v_a/V$
0	0	0	0	3.857
1.25	.944	.892	.944	1.282
2.5	1.400	1.011	1.005	.950
5.0	2.078	1.113	1.055	.688
7.5	2.611	1.167	1.080	.564
10	3.044	1.200	1.095	.486
15	3.744	1.238	1.113	.389
20	4.244	1.256	1.121	.327
30	4.833	1.265	1.124	.249
40	5.000	1.253	1.119	.197
50	4.856	1.235	1.111	.159
60	4.433	1.205	1.098	.127
70	3.733	1.157	1.076	.100
80	2.767	1.089	1.044	.073
90	1.556	.990	.995	.045
95	.856	.910	.954	.030
100	.100	0	0	0
L.E. radius: 0.272 percent c				

Figure 5.- NACA 0010-34 basic thickness form.

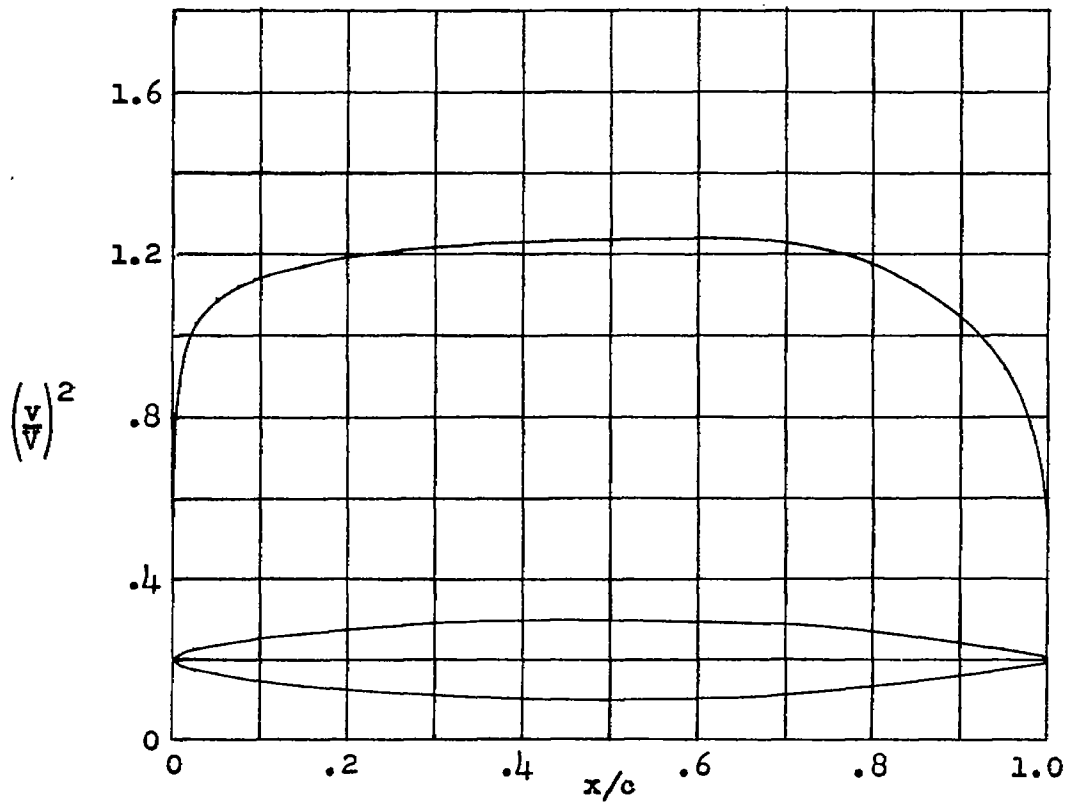

x (percent c)	y (percent c)	$(v/V)^2$	v/V	$\Delta v_a/V$
0	0	0	0	4.068
1.25	.878	.954	.977	1.309
2.5	1.267	1.032	1.016	.952
5.0	1.844	1.087	1.043	.679
7.5	2.289	1.122	1.059	.555
10	2.667	1.141	1.068	.476
15	3.289	1.172	1.083	.382
20	3.789	1.194	1.093	.323
30	4.478	1.214	1.102	.247
40	4.878	1.229	1.109	.198
50	5.000	1.235	1.111	.162
60	4.867	1.240	1.114	.131
70	4.389	1.227	1.108	.104
80	3.500	1.176	1.084	.076
90	2.100	1.046	1.023	.048
95	1.178	.920	.959	.030
100	.100	0	0	0
L.E. radius: 0.272 percent c				

Figure 6.- NACA 0010-35 basic thickness form.

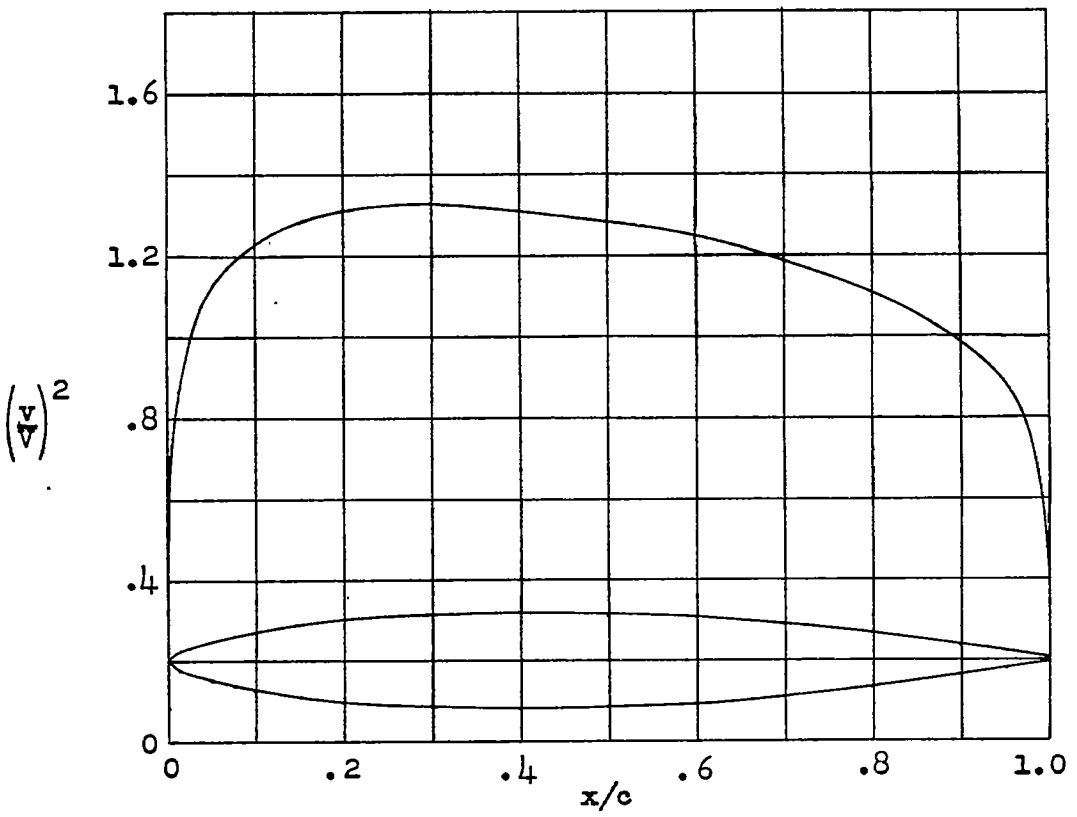

x (percent c)	y (percent c)	$(v/V)^2$	v/V	$\Delta v_a/V$
0	0	0	0	3.154
1.25	1.133	.865	.930	1.251
2.5	1.680	.997	.999	.933
5.0	2.493	1.122	1.059	.683
7.5	3.133	1.186	1.089	.560
10	3.653	1.229	1.109	.484
15	4.493	1.282	1.132	.389
20	5.093	1.310	1.145	.329
30	5.800	1.329	1.153	.250
40	6.000	1.311	1.145	.198
50	5.827	1.284	1.133	.158
60	5.320	1.249	1.118	.128
70	4.480	1.192	1.092	.098
80	3.320	1.112	1.055	.071
90	1.867	.985	.992	.045
95	1.027	.894	.946	.029
100	.120	0	0	0
L.E. radius: 0.391 percent c				

Figure 7.- NACA 0012-34 basic thickness form.

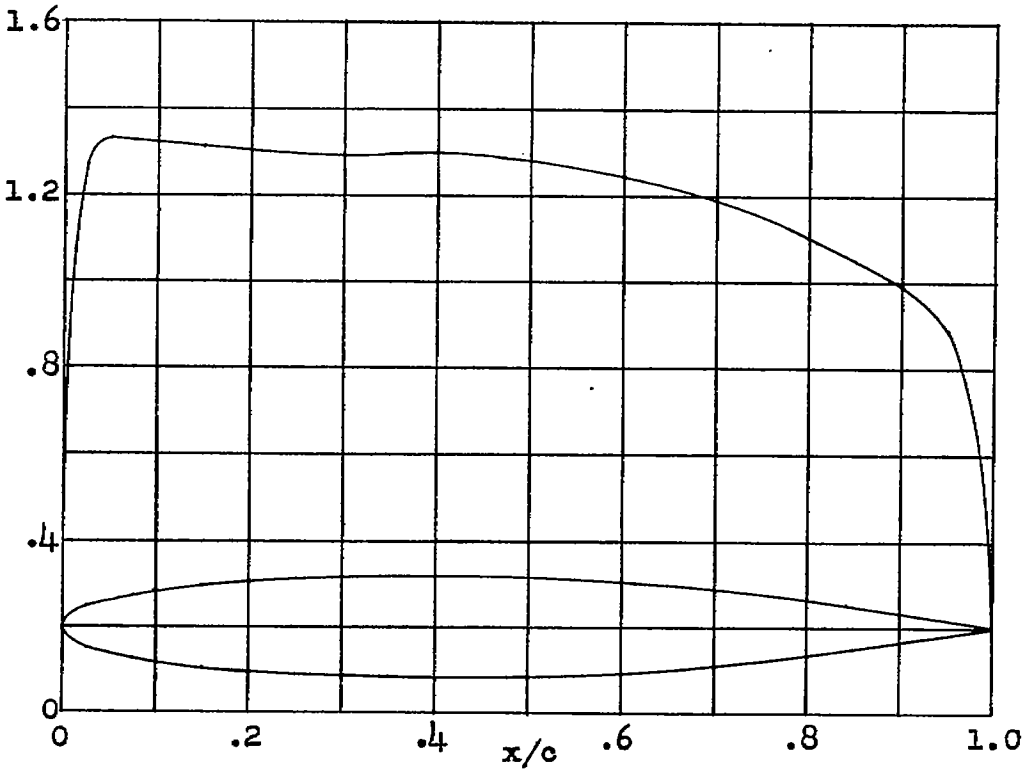

x (percent c)	y (percent c)	$(v/V)^2$	v/V	$\Delta v_a/V$
0	0	0	0	2.019
1.25	1.813	1.072	1.035	1.236
2.5	2.453	1.270	1.127	.952
5.0	3.267	1.330	1.153	.685
7.5	3.813	1.325	1.151	.554
10	4.240	1.322	1.150	.474
15	4.867	1.313	1.146	.372
20	5.293	1.303	1.141	.315
30	5.827	1.297	1.139	.241
40	6.000	1.300	1.140	.199
50	5.827	1.280	1.131	.154
60	5.320	1.244	1.115	.126
70	4.480	1.189	1.090	.096
80	3.320	1.102	1.050	.070
90	1.867	.993	.996	.044
95	1.027	.889	.943	.028
100	.120	0	0	0
L.E. radius: 1.582 percent c				

Figure 8.- NACA 0012-64 basic thickness form.

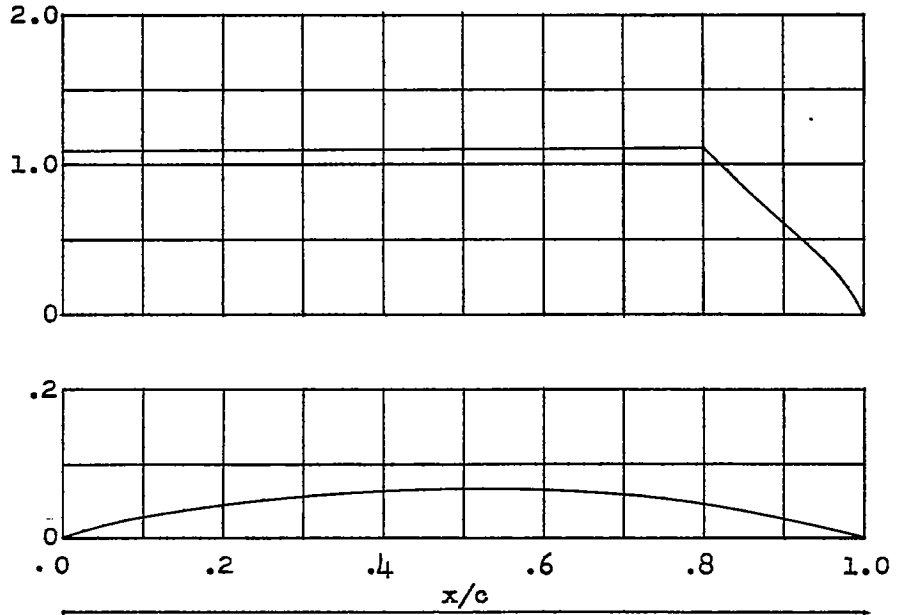

$c_{l_i} = 1.0$ $\quad \alpha_i = 1.40°$ $\quad c_{m_{c/4}} = 0.219$

x (percent c)	y_c (percent c)	dy_c/dx	P_R	$\Delta v/V = P_R/4$
0	0	-------	-----	-----
.5	.281	0.47539		
.75	.396	.44004		
1.25	.603	.39531		
2.5	1.055	.33404	1.092	0.273
5.0	1.803	.27149		
7.5	2.432	.23378		
10	2.981	.20618		
15	3.903	.16546		
20	4.651	.13452		
25	5.257	.10873	1.096	.274
30	5.742	.08595		
35	6.120	.06498		
40	6.394	.04507	1.100	.275
45	6.571	.02559		
50	6.651	.00607		
55	6.631	-.01404	1.104	.276
60	6.508	-.03537		
65	6.274	-.05887	1.108	.277
70	5.913	-.08610	1.108	.277
75	5.401	-.12058	1.112	.278
80	4.673	-.18034	1.112	.278
85	3.607	-.23430	.840	.210
90	2.452	-.24521	.588	.147
95	1.226	-.24521	.368	.092
100	0	-.24521	0	0

Figure 9.- Data for NACA mean line a = 0.8 (modified).

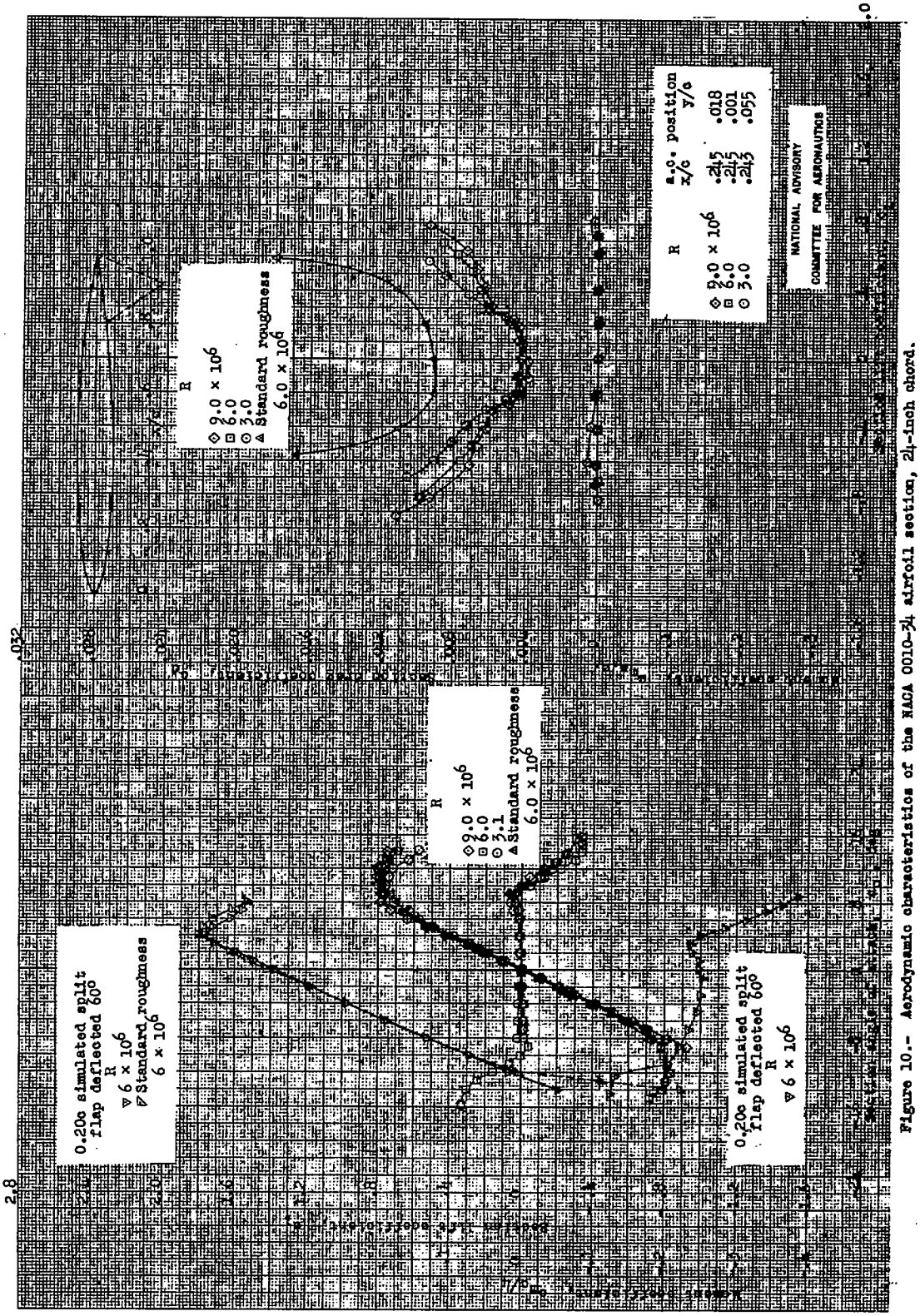

Figure 10.- Aerodynamic characteristics of the NACA 0010-34 airfoil section, 24-inch chord.

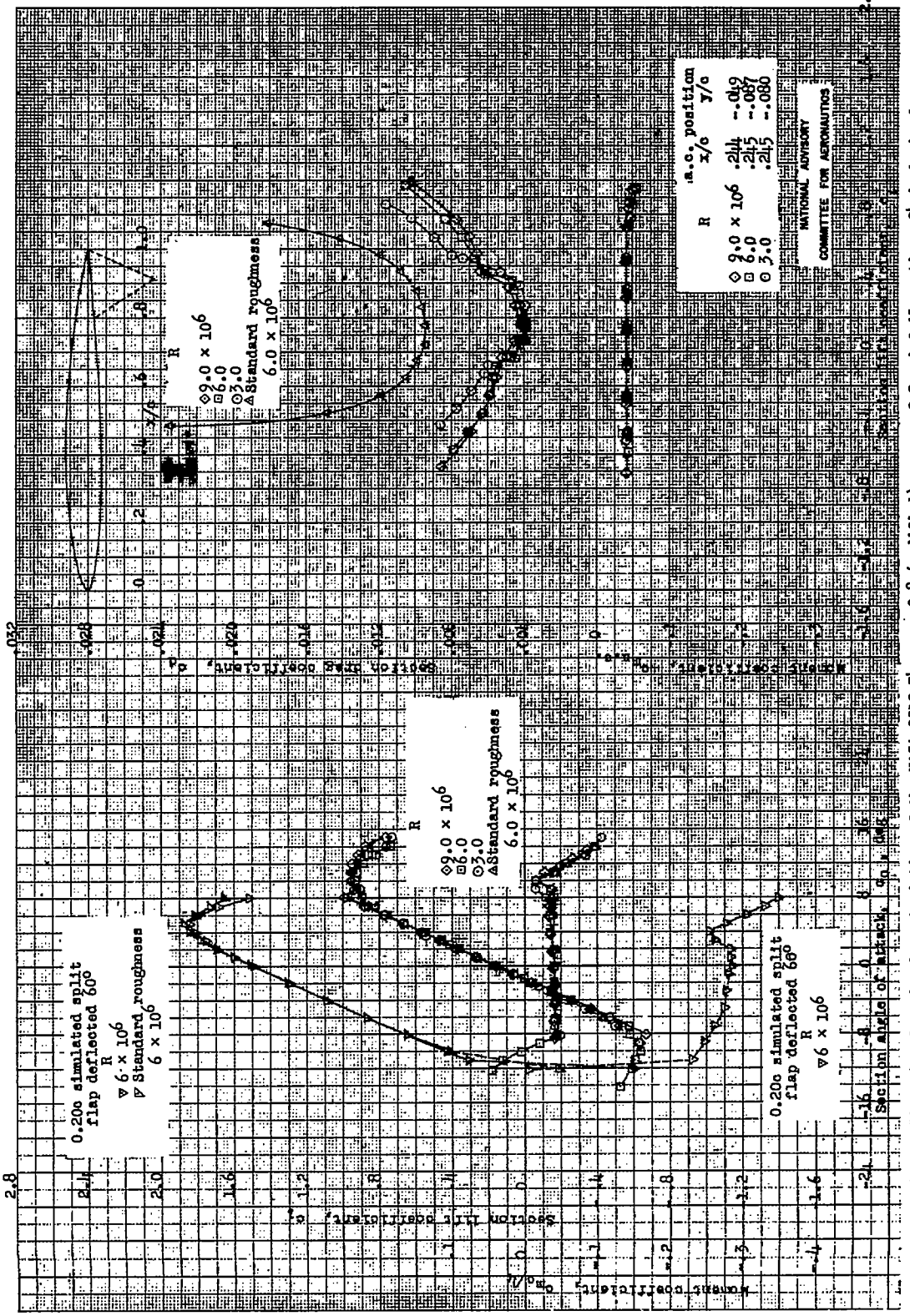

Figure 11.- Aerodynamic characteristics of the NACA 0010-34, a = 0.8 (modified), $\alpha_{t_1} = 0.2$ airfoil section, 24-inch chord:

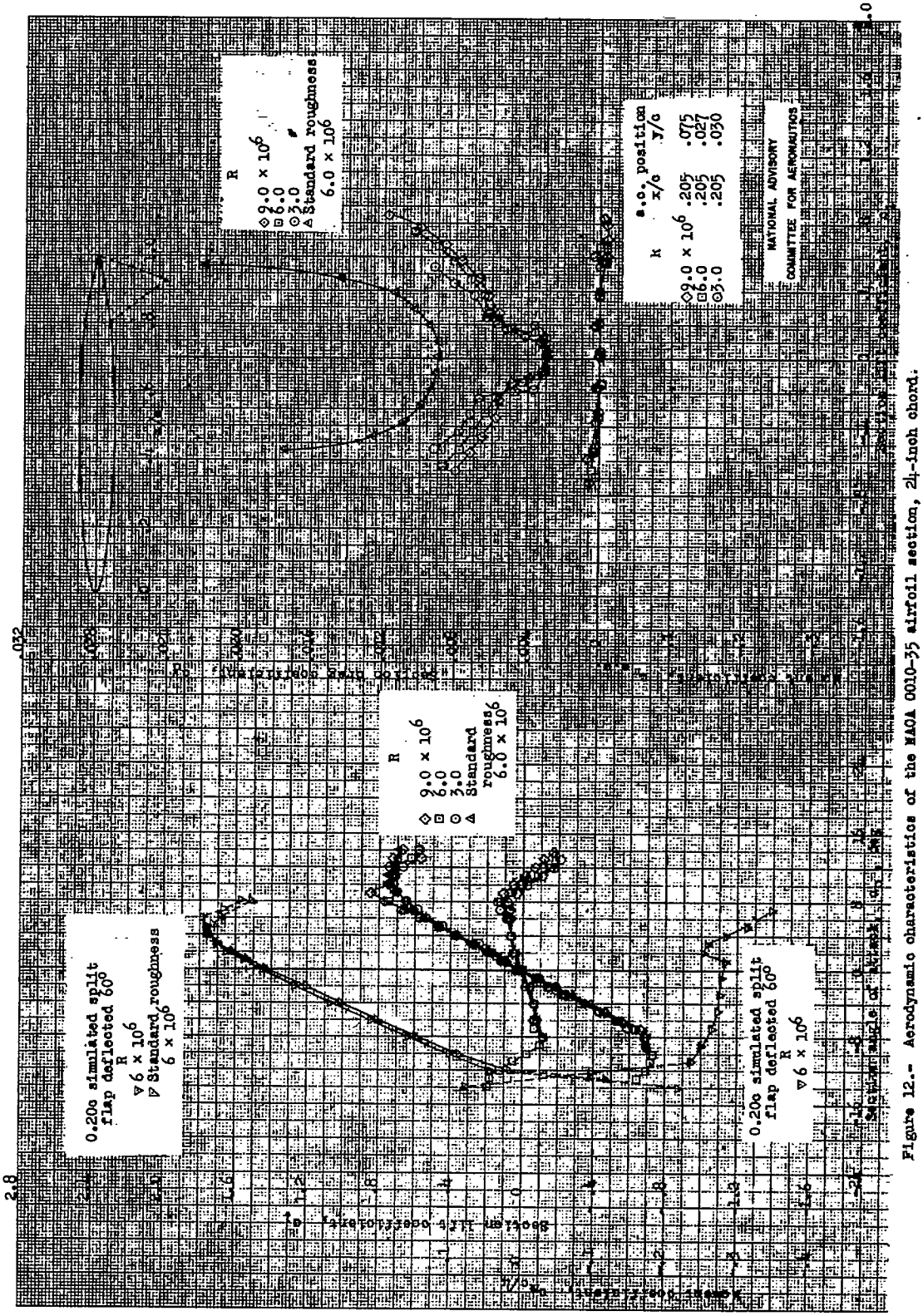

Figure 12.- Aerodynamic characteristics of the NACA 0010-35 airfoil section, 24-inch chord.

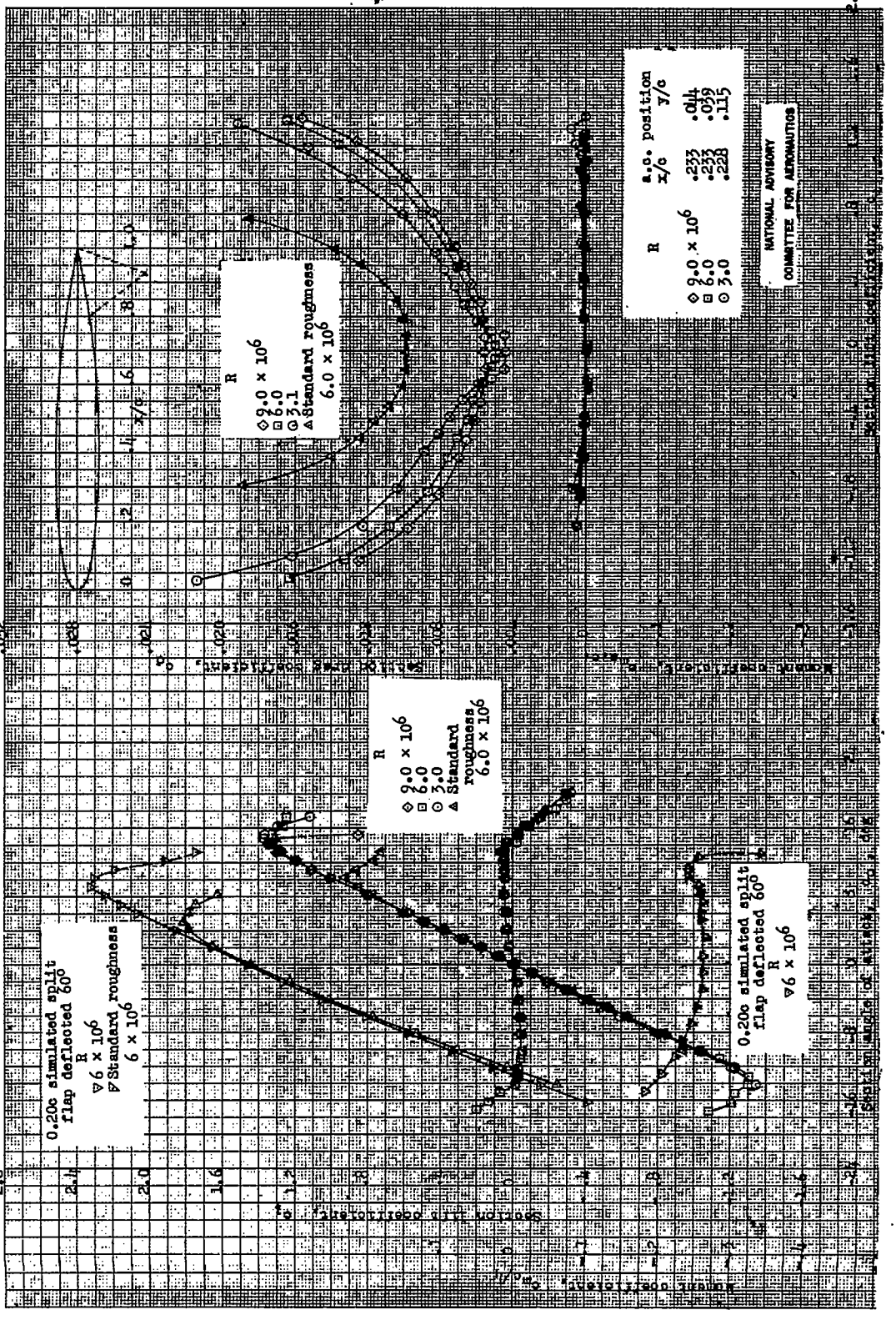

Figure 13.- Aerodynamic characteristics of the NACA 0012-64 airfoil section, 24-inch chord.

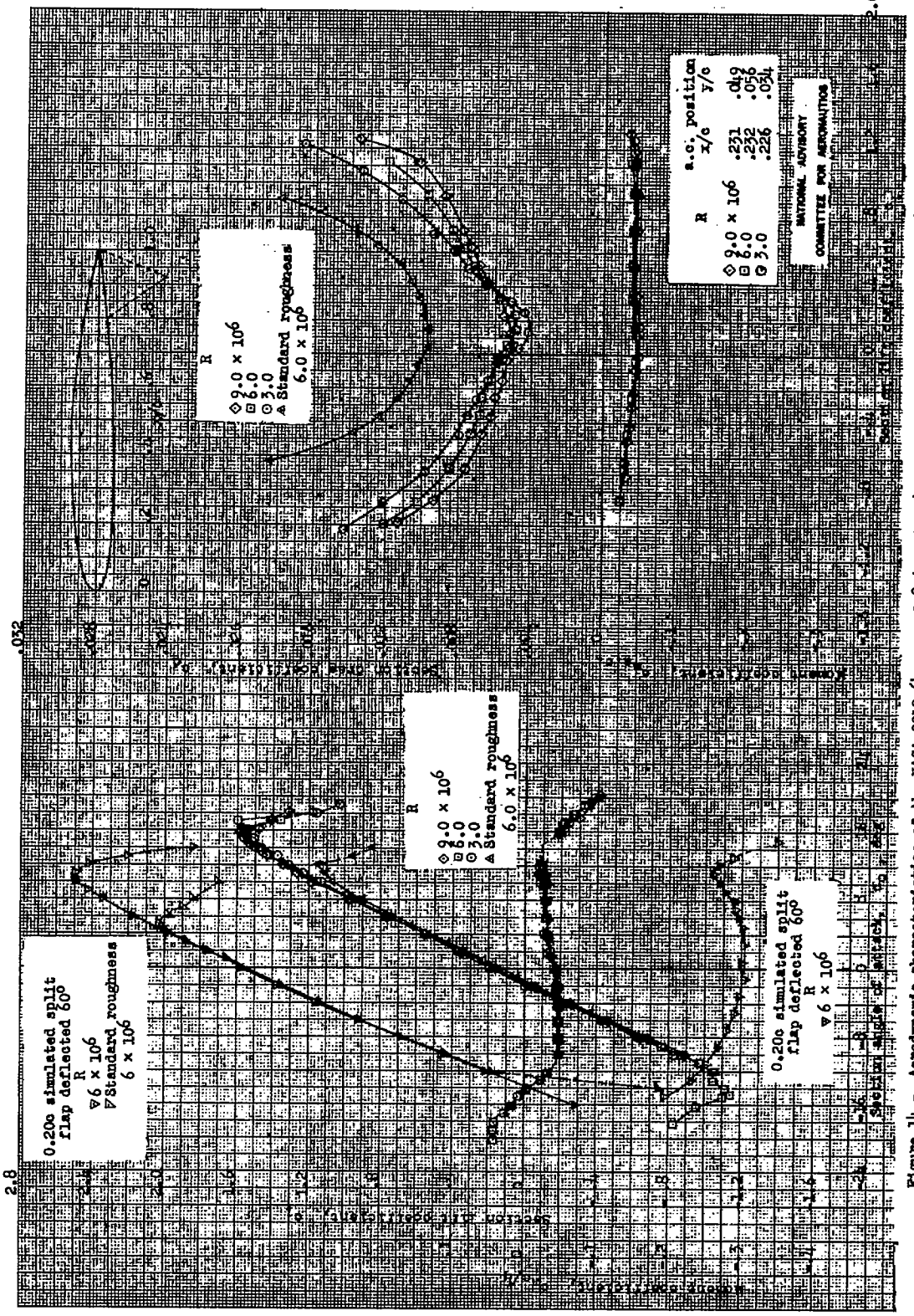

Figure 14.- Aerodynamic characteristics of the NACA 0012-64, a = 0.8 (modified), c_{l_1} = 0.2 airfoil section, 24-inch chord.

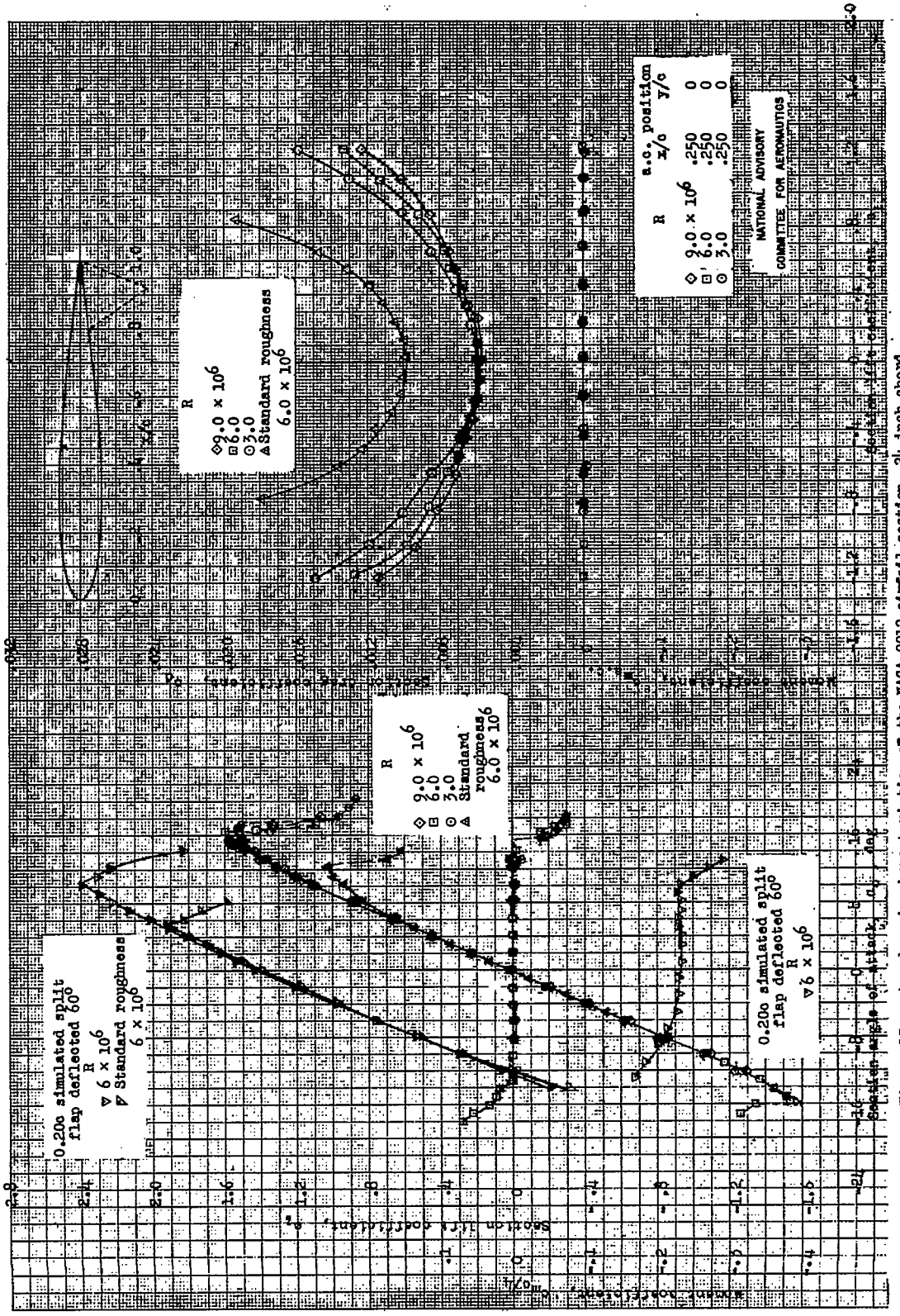

Figure 15.- Aerodynamic characteristics of the NACA 0012 airfoil section, 24-inch chord.

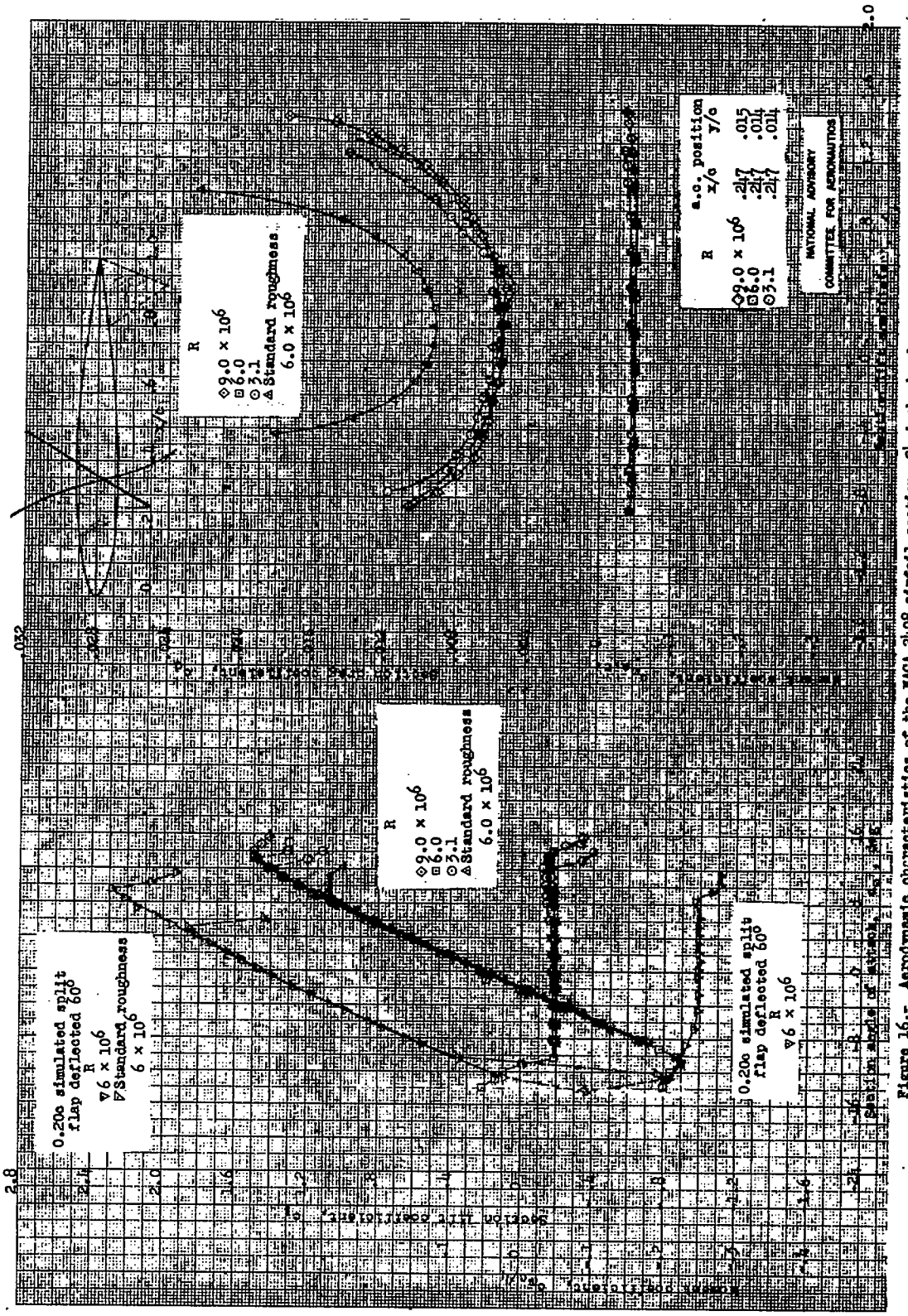

Figure 16.- Aerodynamic characteristics of the NACA 2408 airfoil section, 24-inch chord.

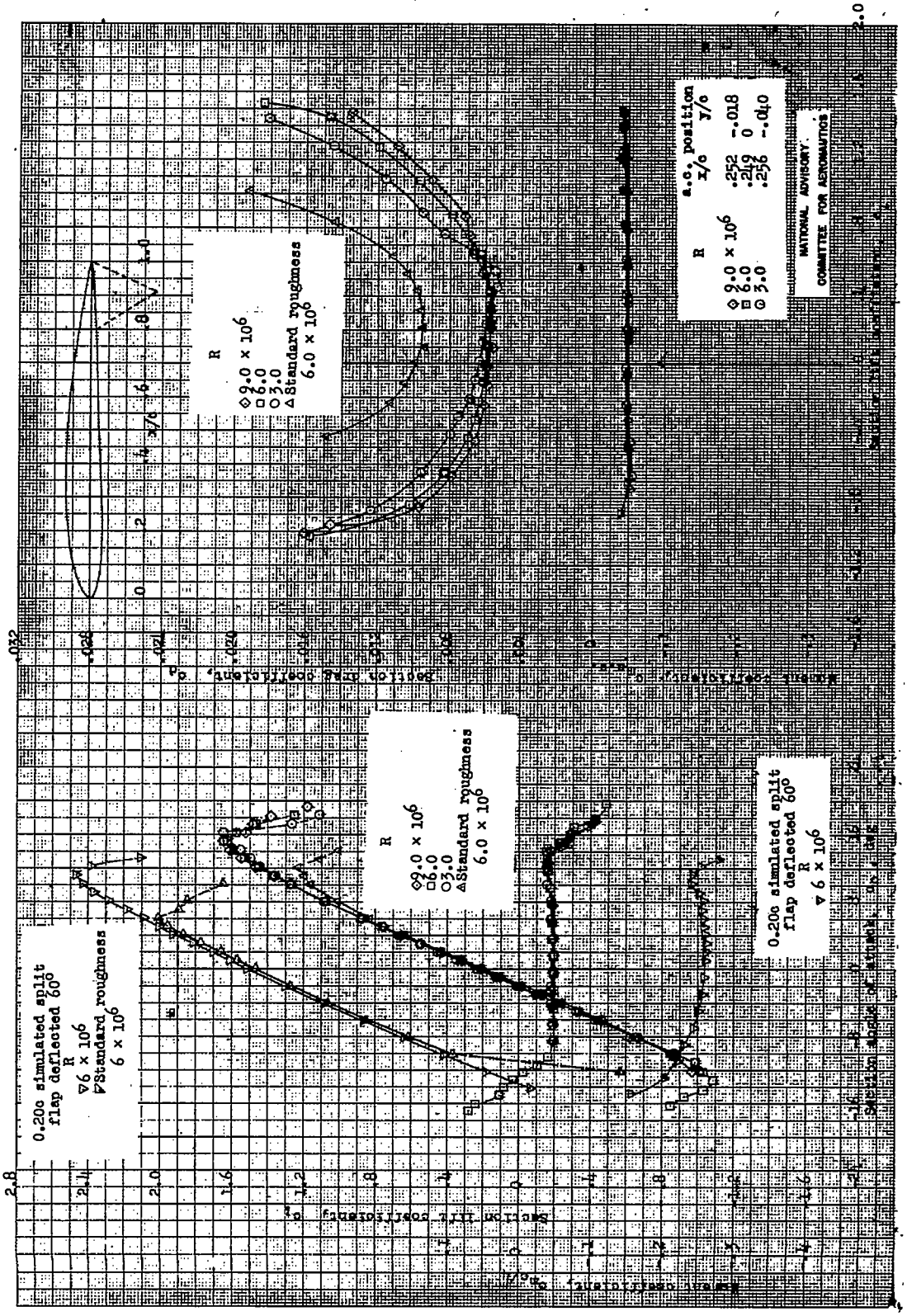

Figure 17.- Aerodynamic characteristics of the NACA 2410 airfoil section, 24-inch chord.

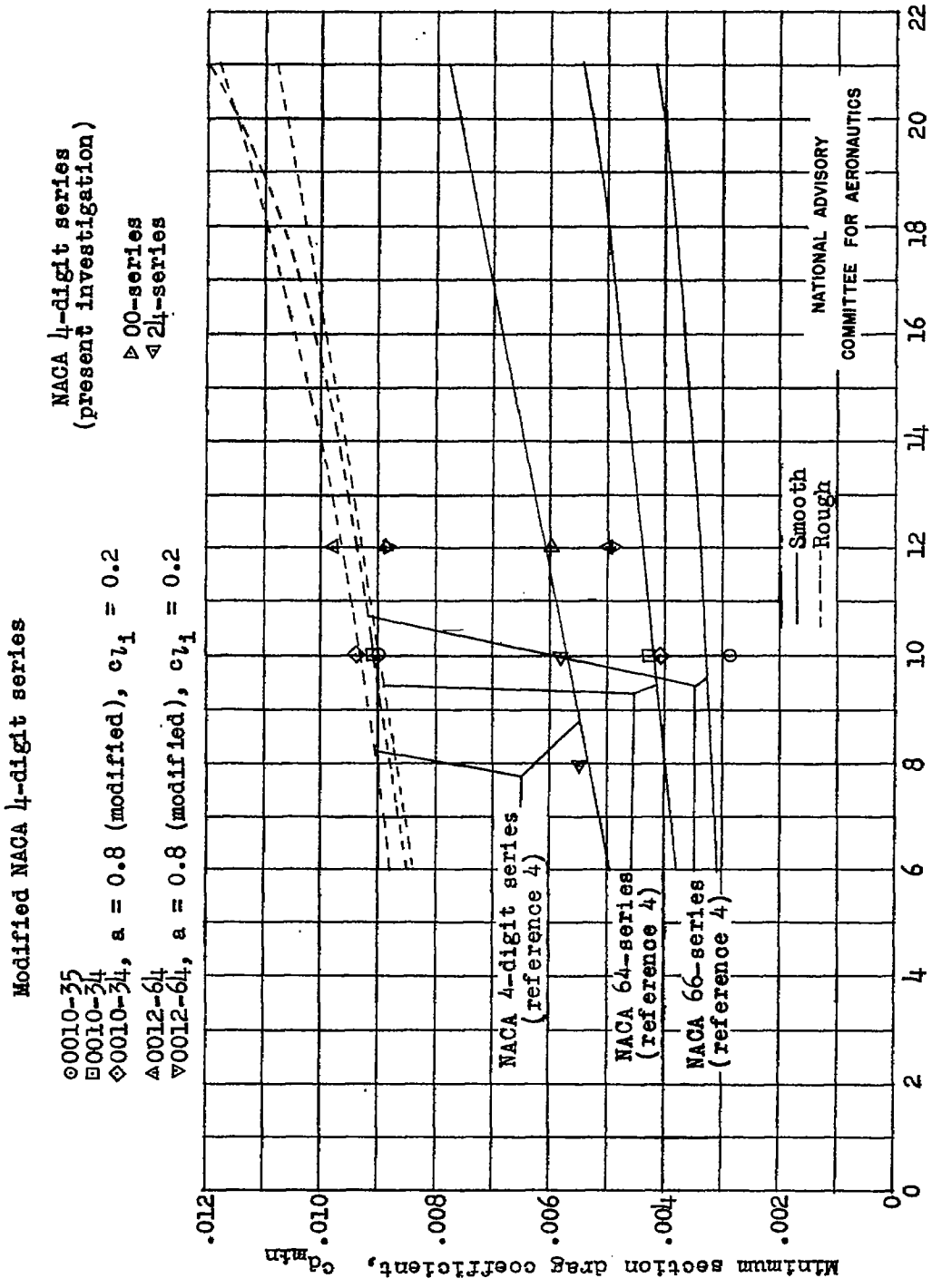

Figure 18.- Minimum section drag coefficients of several modified NACA four-digit-series airfoil sections, both with and without standard roughness, as compared with those of a number of NACA 6-series and NACA four-digit-series airfoil sections. R = 6.0 x 10^6.

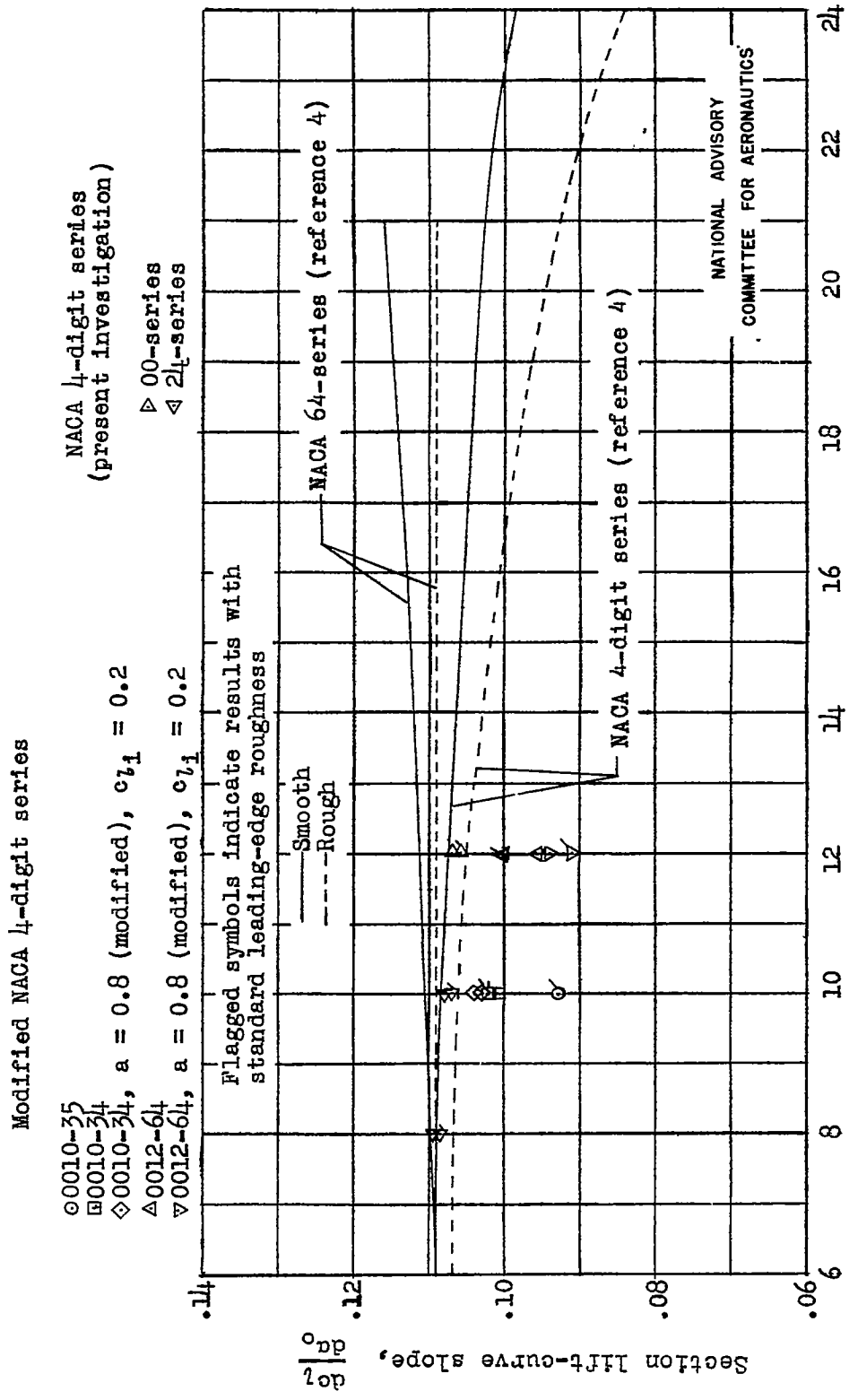

Figure 19.- Section lift-curve slopes of several modified NACA four-digit-series airfoil sections, both with and without standard roughness, as compared with those of a number of NACA 64-series and NACA four-digit-series airfoil sections. $R = 6.0 \times 10^6$.

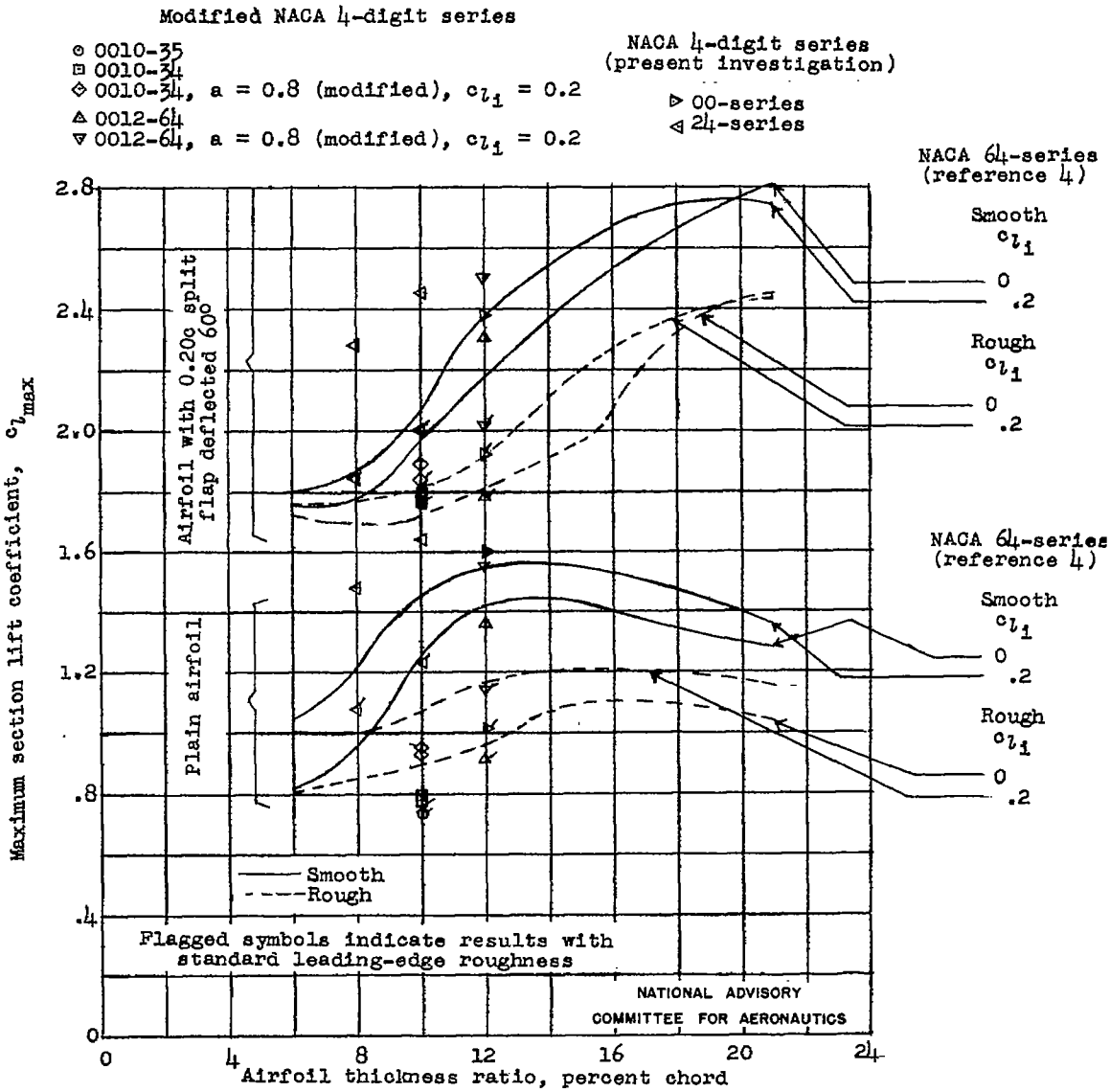

Figure 20.- Maximum section lift coefficients of several modified NACA four-digit-series airfoil sections, both with and without standard roughness and split flaps, as compared with those of a number of NACA 64-series and NACA four-digit-series airfoil sections. R = 6.0×10^6.

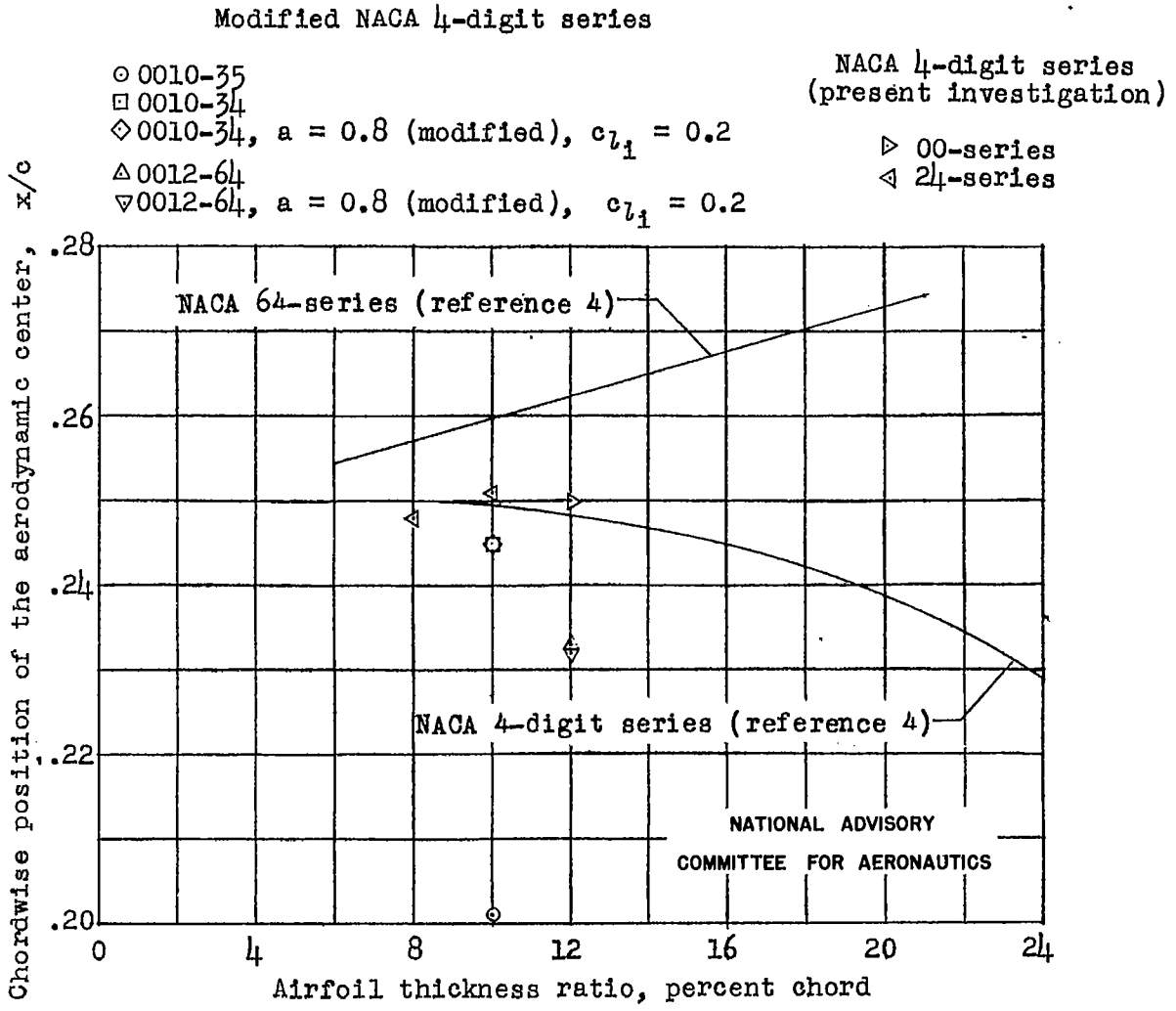

Figure 21.- Chordwise position of the aerodynamic center of several modified NACA four-digit-series airfoil sections as compared with those of a number of NACA 64-series and NACA four-digit-series airfoil sections. R = 6.0 x 10^6.